Part I

Configuration

Chapter 2

Governing Equations

In this chapter, the governing equations for the general ocean circulation are formulated. These equations are usually called primitive equations. A discrete form of these equations is also presented to explain the fundamental solution methods. The detailed numerical methods are presented in later chapters.

2.1 Formulation

2.1.1 Coordinate System

The fundamental purpose of developing this ocean circulation model (MRI.COM) is to use it for realistic simulations of oceanic circulations in various circumstances. To achieve this, we must carefully choose a coordinate system before formulating the governing equations.

In the lateral direction, the governing equations need to be formulated on a sphere. Originally, spherical coordinates were adopted, and the equations were discretized on a geographical (latitude-longitude-depth) grid. A problem arises for a global model because the North Pole is a singular point in the geographic coordinate system. Since the zonal grid widths within five latitudinal degrees from the Pole become less than a tenth of those in middle to low latitudes, a short time step is required owing to the limitation of the Courant-Friedrichs-Lewy (CFL) condition.[*] This becomes a burden on performing long-term integration.

One simple means to remove this North Pole singularity is to shift both poles to land. In this case, one may use the spherical coordinate program codes without major modification by only adjusting the Coriolis parameter. Unfortunately, there are not many pairs of points on land that are symmetric about the Earth's center.[†] Even if the most ideal pair with poles on Greenland and Antarctica (near the Ross Sea) was chosen, it is only 5 degrees from the coastline to the newly shifted pole. One might also be concerned that the Equator is not represented as a line on the shifted grid arrangement.[‡]

To resolve these issues, the model equations are represented on generalized orthogonal coordinates instead of spherical coordinates. Users can select the coordinate system according to their purposes. For example, the resolution of a target region can be intentionally enhanced by placing a pole of the distorted grid near the target region. Of course, a regional model without the North Pole may be arranged on geographic coordinates since spherical coordinates are one form of generalized orthogonal coordinates. Now our model equations are formulated on generalized orthogonal coordinates. Chapter 24 summarizes the concepts and calculus related to generalized orthogonal coordinates.

In the vertical direction, the depth coordinate was adopted from the first stage of the development. No attempt has been made to apply other options such as terrain following or density coordinates. In the earliest stage, the sea surface was assumed to have a rigid-lid on it. Then, the sea surface was allowed to move freely. When the free surface was first introduced, the movement of sea surface was absorbed in the first layer of the model. The problem with this treatment is that it is not possible to take the first layer thickness thinner than about 4 meters whereas a finer vertical resolution is required near the sea surface. This is because the contrast of mean sea level in the global ocean may reach 3 meters. To resolve this problem, the upper several layers were allowed to undulate following the sea surface evolution as in the sigma-coordinate model (Hasumi, 2006). A problem with this approach is that there is a transition in the vertical coordinate, which would make analytical treatment awkward in some situations. For MRI.COM version 4, we have adopted a vertically rescaled height coordinate system, where a sea level undulation is reflected throughout the water column (Adcroft and Campin, 2004). This vertical coordinate is named z^* coordinate.

In this section, we first formulate the governing equations on Cartesian coordinates for brevity. Then a coordinate transformation in the lateral direction is applied to the governing equations. Approximations and boundary conditions

---

[*] The time step, Δt, needs to satisfy $v\Delta t/\Delta x \leq 1$, where v is velocity and Δx is the grid width.

[†] Greenland and Antarctica, China and Argentina, Kalimantan and Columbia.

[‡] If the grid size is fine enough, the Kelvin wave in the shifted-pole model will propagate along the Equator as the theory suggests.

are discussed using equations on generalized orthogonal coordinates. Equations are further transformed to introduce generalized vertical coordinates. Readers are referred to Griffies and Adcroft (2008) for the thorough discussion on the formulation of primitive equations for ocean circulation models.

2.1.2 Primitive equations in Cartesian coordinates

a. General governing equations

Evolution of state variables of ocean circulation $(\mathbf{v}, \rho, \theta, S, p)$, where $\mathbf{v} = (u, v, w)$ is the velocity vector, ρ is density, θ is potential temperature, S is salinity, and p is pressure, is obtained by solving the following simultaneous equations written in Cartesian coordinates.

Momentum equation in a vector form is

$$\rho \frac{\partial \mathbf{v}}{\partial t} + \rho (\mathbf{v} \cdot \nabla) \mathbf{v} + 2\Omega \times (\rho \mathbf{v}) = -\rho \nabla \Phi - \nabla p + \nabla \cdot \tau, \tag{2.1}$$

where Ω is the rotation vector of the Earth, Φ is the geopotential, τ is the frictional stress tensor.

Mass conservation equation is

$$\frac{\partial \rho}{\partial t} + \nabla \cdot (\rho \mathbf{v}) = 0. \tag{2.2}$$

Equations for potential temperature and salinity are

$$\rho \frac{\partial \theta}{\partial t} + \rho \mathbf{v} \cdot \nabla \theta = -\nabla \cdot (\rho \mathbf{F}^\theta) + \rho Q^\theta \tag{2.3}$$

and

$$\rho \frac{\partial S}{\partial t} + \rho \mathbf{v} \cdot \nabla S = -\nabla \cdot (\rho \mathbf{F}^S) + \rho Q^S, \tag{2.4}$$

where $\mathbf{F}^{\theta,S}$ are tracer fluxes due to subgrid-scale transport and mixing parameterizations and $Q^{\theta,S}$ are sources of tracers due to nudging, convective adjustment (Section 12.2), shortwave absorption (Section 14.3), etc. Here, tracer concentration is expressed as concentration per unit mass of sea water.

Equation of state of sea water determines in situ density of sea water. Density is given as a function of potential temperature, salinity, and pressure:

$$\rho = \rho(\theta, S, p). \tag{2.5}$$

The equation of state is usually given as a polynomial fit to the available measurements. A detailed description of this will be presented in Chapter 5.

The above set is the most general set of equations governing the evolution of oceanic state.

b. Boussinesq approximation

Because the density of sea water varies only by 5% throughout the water column and the horizontal density variations are less than 1%, most ocean general circulation models use the Boussinesq approximation. In the Boussinesq approximation, the density (ρ) in the non-linear product of density times velocity ($\rho \mathbf{v}$) that appears in the momentum equation (2.1) is replaced by a reference density (ρ_0). The momentum equation becomes

$$\frac{\partial \mathbf{v}}{\partial t} + (\mathbf{v} \cdot \nabla) \mathbf{v} + 2\Omega \times \mathbf{v} = -\frac{\rho}{\rho_0} \nabla \Phi - \frac{1}{\rho_0} \nabla p + \frac{1}{\rho_0} \nabla \cdot \tau. \tag{2.6}$$

Note that the in-situ density (ρ) is retained for the geopotential term.

Further, the sea water is treated as incompressible. Mass conservation equation (2.2) becomes the volume conservation equation:

$$\nabla \cdot \mathbf{v} = 0. \tag{2.7}$$

The tracer concentrations are now concentration per unit volume instead of unit mass:

$$\frac{\partial \theta}{\partial t} + \mathbf{v} \cdot \nabla \theta = -\nabla \cdot \mathbf{F}^\theta + Q^\theta, \tag{2.8}$$

and

$$\frac{\partial S}{\partial t} + \mathbf{v} \cdot \nabla S = -\nabla \cdot \mathbf{F}^S + Q^S. \tag{2.9}$$

The above expression is the most general form under the Boussinesq approximation. This form is used to formulate an oceanic non-hydrostatic model and a quasi-hydrostatic model (Marshall et al., 1997).

2.1.3   Primitive equations in generalized orthogonal coordinates

We consider the momentum equation first. On a generalized orthogonal coordinate system (μ, ψ, r) whose unit vectors are $\mathbf{e}_\mu$, $\mathbf{e}_\psi$, and $\mathbf{e}_r$, the momentum equation for velocity $\mathbf{v} = u\mathbf{e}_\mu + v\mathbf{e}_\psi + w\mathbf{e}_r$, where $u = h_\mu \dot{\mu}$, $v = h_\psi \dot{\psi}$, $w = h_r \dot{r}$, is represented by

$$\frac{\partial u}{\partial t} + \mathbf{v} \cdot \nabla u + f_\psi w - f v = -\frac{1}{\rho_0 h_\mu} \frac{\partial p}{\partial \mu} - \frac{v}{h_\mu h_\psi} \left(\frac{\partial h_\mu}{\partial \psi} u - \frac{\partial h_\psi}{\partial \mu} v \right) - \frac{w}{h_r h_\mu} \left(\frac{\partial h_\mu}{\partial r} u - \frac{\partial h_r}{\partial \mu} w \right) + F_{\text{fric}}^\mu, \tag{2.10}$$

$$\frac{\partial v}{\partial t} + \mathbf{v} \cdot \nabla v + f u - f_\mu w = -\frac{1}{\rho_0 h_\psi} \frac{\partial p}{\partial \psi} - \frac{w}{h_\psi h_r} \left(\frac{\partial h_\psi}{\partial r} v - \frac{\partial h_r}{\partial \psi} w \right) - \frac{u}{h_\mu h_\psi} \left(\frac{\partial h_\psi}{\partial \mu} v - \frac{\partial h_\mu}{\partial \psi} u \right) + F_{\text{fric}}^\psi, \tag{2.11}$$

$$\frac{\partial w}{\partial t} + \mathbf{v} \cdot \nabla w + f_\mu v - f_\psi u = -\frac{1}{\rho_0 h_r} \frac{\partial p}{\partial r} - \frac{\rho}{\rho_0} \frac{\partial \Phi}{\partial r} - \frac{u}{h_r h_\mu} \left(\frac{\partial h_r}{\partial \mu} w - \frac{\partial h_\mu}{\partial r} u \right) - \frac{v}{h_\psi h_r} \left(\frac{\partial h_r}{\partial \psi} w - \frac{\partial h_\psi}{\partial r} v \right) + F_{\text{fric}}^r, \tag{2.12}$$

where h_μ, h_ψ, and h_r are scale factors, which measure the width in the original coordinate of the unit length in the new coordinate. Metric terms appear on the r.h.s.. $\mathbf{F}_{\text{fric}}$ is frictional force obtained as the divergence of frictional stress tensor. The radial distance from the Earth's center is represented by r and the gravitational acceleration is in the negative direction of r.

   The Coriolis force is represented by

$$2\Omega \times \mathbf{v} = (2\Omega_\psi w - 2\Omega_r v)\mathbf{e}_\mu + (2\Omega_r u - 2\Omega_\mu w)\mathbf{e}_\psi + (2\Omega_\mu v - 2\Omega_\psi u)\mathbf{e}_r, \tag{2.13}$$

where $\Omega = \Omega_\mu \mathbf{e}_\mu + \Omega_\psi \mathbf{e}_\psi + \Omega_r \mathbf{e}_r$ is the rotation vector of the Earth. We designate $f_\mu = 2\Omega_\mu$, $f_\psi = 2\Omega_\psi$, and $f = f_r = 2\Omega_r$.

   We apply the following two approximations which are relevant to the momentum equation.

a. Shallow ocean approximation

Shallow ocean approximation employs the fact that the vertical thickness of the ocean is far smaller than the radius of the Earth. Since the vertical scale of motion of a water particle is far smaller than the Earth's radius (a), the radial distance r as a scalar quantity is replaced by the Earth's radius a. The new vertical coordinate (z) is the distance (positive upward) from the geoid (sea surface height in the state of rest) and $\partial/\partial r$ is replaced by $\partial/\partial z$. We set a constant vertical scale factor $h_r (= h_z = 1)$. Horizontal scale factors are independent of vertical coordinate $(\partial h_\mu/\partial r = \partial h_\psi/\partial r = 0)$. As a result, to conserve angular momentum under this approximation, we drop the metric terms that involve w for the horizontal components and all the metric terms for the vertical components.

   We also assume that the gravitational acceleration is constant (g). This assumption results in a specific expression of geopotential as $\Phi = gz$.

b. Hydrostatic approximation

For horizontal motions with a scale larger than a few kilometers, hydrostatic balance is maintained in the vertical direction. The vertical momentum equation becomes:

$$0 = -\frac{\partial p}{\partial z} - \rho g. \tag{2.14}$$

   By hydrostatic approximation, we must drop all the remaining Coriolis terms that do not involve f to conserve angular momentum (Phillips, 1966).

   We also separately treat horizontal and vertical strain for calculating frictional stresses. The vertical stress is usually parameterized as the vertical diffusion of momentum:

$$\mathbf{F}_{\text{fric}} = \frac{1}{\rho_0} \nabla \cdot \tau = \frac{\partial}{\partial z} \left(\nu_V \frac{\partial \mathbf{u}}{\partial z} \right) + \frac{1}{\rho_0} \nabla \cdot \tau_{\text{horizontal strain}}, \tag{2.15}$$

where ν_V is the vertical viscosity (essentially vertical diffusion of momentum).

c. Equations solved by a standard version of MRI.COM

With the above approximations, the momentum equation is now written as:

$$\frac{\partial u}{\partial t} + \frac{1}{h_\mu h_\psi} \left\{ \frac{\partial(h_\psi uu)}{\partial \mu} + \frac{\partial(h_\mu vu)}{\partial \psi} \right\} + \frac{\partial(wu)}{\partial z} + \frac{v}{h_\mu h_\psi} \left(\frac{\partial h_\mu}{\partial \psi} u - \frac{\partial h_\psi}{\partial \mu} v \right) - fv$$
$$= -\frac{1}{\rho_0 h_\mu} \frac{\partial p}{\partial \mu} + \frac{1}{\rho_0} (\nabla \cdot \tau_{\text{horizontal strain}})_u + \frac{\partial}{\partial z} \left(\nu_V \frac{\partial u}{\partial z} \right), \tag{2.16}$$

$$\frac{\partial v}{\partial t} + \frac{1}{h_\mu h_\psi} \left\{ \frac{\partial(h_\psi uv)}{\partial \mu} + \frac{\partial(h_\mu vv)}{\partial \psi} \right\} + \frac{\partial(wv)}{\partial z} + \frac{u}{h_\mu h_\psi} \left(\frac{\partial h_\psi}{\partial \mu} v - \frac{\partial h_\mu}{\partial \psi} u \right) + fu$$
$$= -\frac{1}{\rho_0 h_\psi} \frac{\partial p}{\partial \psi} + \frac{1}{\rho_0} (\nabla \cdot \tau_{\text{horizontal strain}})_v + \frac{\partial}{\partial z} \left(\nu_V \frac{\partial v}{\partial z} \right). \tag{2.17}$$

Continuity equation is written as:

$$\frac{1}{h_\mu h_\psi} \left\{ \frac{\partial(h_\psi u)}{\partial \mu} + \frac{\partial(h_\mu v)}{\partial \psi} \right\} + \frac{\partial w}{\partial z} = 0. \tag{2.18}$$

The equations for potential temperature and salinity are written as:

$$\frac{\partial \theta}{\partial t} = -\frac{1}{h_\mu h_\psi} \left\{ \frac{\partial(h_\psi u\theta)}{\partial \mu} + \frac{\partial(h_\mu v\theta)}{\partial \psi} \right\} - \frac{\partial(w\theta)}{\partial z} - \nabla \cdot \mathbf{F}^\theta + Q^\theta, \tag{2.19}$$

$$\frac{\partial S}{\partial t} = -\frac{1}{h_\mu h_\psi} \left\{ \frac{\partial(h_\psi uS)}{\partial \mu} + \frac{\partial(h_\mu vS)}{\partial \psi} \right\} - \frac{\partial(wS)}{\partial z} - \nabla \cdot \mathbf{F}^S + Q^S. \tag{2.20}$$

2.1.4 Boundary conditions

a. Momentum equation

■ Upper surface ($z = \eta$):   At the sea surface, momentum flux enters the ocean in the form of wind stress (or stress from sea ice where sea ice exists):

$$\nu_V \frac{\partial(u,v)}{\partial z} \bigg|_{z=\eta} = \frac{(\tau^\mu, \tau^\psi)}{\rho_0}. \tag{2.21}$$

Note that z is defined positive upward (the surface wind stress is positive into the ocean).
   In the model algorithm, this is treated as a body force to the first level velocity. See Chapter 14 for details.
   Surface fresh water flux is assumed to have zero velocity.

■ Bottom ($z = -H$):   Bottom friction (τ_b^μ in zonal and τ_b^ψ in meridional direction) exists at the sea floor ($z = -H(\mu, \psi)$).

$$\nu_V \frac{\partial(u,v)}{\partial z} \bigg|_{z=-H(\mu,\psi)} = -\frac{(\tau_b^\mu, \tau_b^\psi)}{\rho_0}. \tag{2.22}$$

   In the model algorithm, this is treated as a body force to the bottom level ($k = \text{kbtm}$) velocity. See Chapter 8 for details.

■ Side wall: No slip condition is applied ($u = v = 0$).

b. Temperature and Salinity

■ Upper surface ($z = \eta$):   At the sea surface, heat and fresh water are exchanged with atmosphere and sea ice. Salt is also exchanged below sea ice. All these exchanges are expressed as surface fluxes and become surface boundary conditions.
   The surface boundary conditions for temperature and salinity are expressed as follows:

$$\kappa_V \frac{\partial \theta}{\partial z} \bigg|_{z=\eta} = F_{\text{surf}}^\theta, \tag{2.23}$$

$$\kappa_V \frac{\partial S}{\partial z} \bigg|_{z=\eta} = F_{\text{surf}}^S, \tag{2.24}$$

where surface flux (F_{surf}^α) is defined positive downward (positive into the ocean).

■ Bottom ($z = -H$):   At the sea floor ($z = -H(\mu, \psi)$), geothermal heating ($F^{\theta}_{\text{bottom}}$) and sediment trap ($F^{S}_{\text{bottom}}$) may affect temperature and salinity:

$$-\kappa_V \left.\frac{\partial \theta}{\partial z}\right|_{z=-H(\mu,\psi)} = F^{\theta}_{\text{bottom}}, \quad -\kappa_V \left.\frac{\partial S}{\partial z}\right|_{z=-H(\mu,\psi)} = F^{S}_{\text{bottom}}, \tag{2.25}$$

where bottom flux ($F^{\alpha}_{\text{bottom}}$) is defined positive upward (positive into the ocean).

■ Side wall: For any tracer, the adiabatic condition is applied at the side wall:

$$\frac{\partial \theta}{\partial n} = 0, \quad \frac{\partial S}{\partial n} = 0, \tag{2.26}$$

where n denotes the direction perpendicular to the wall. River discharge is expressed as a part of the surface fresh water flux.

c. Continuity equation

■ Upper surface ($z = \eta$):   At the sea surface, vertical velocity is generated because a water parcel moves following the freely moving sea surface. Surface fresh water flux is explicitly incorporated into the boundary condition for the continuity equation.

$$w = \frac{d\eta}{dt} - (P - E + R + I) = \frac{\partial \eta}{\partial t} + u\frac{1}{h_\mu}\frac{\partial \eta}{\partial \mu} + v\frac{1}{h_\psi}\frac{\partial \eta}{\partial \psi} - (P - E + R + I), \tag{2.27}$$

where P is precipitation, E is evaporation, R is river discharge, and I is fresh water exchange with sea ice component.

■ Bottom ($z = -H$):   At the sea floor, vertical velocity is generated because the water parcel moves following the bottom topography:

$$w = -\left(u\frac{1}{h_\mu}\frac{\partial H}{\partial \mu} + v\frac{1}{h_\psi}\frac{\partial H}{\partial \psi}\right). \tag{2.28}$$

■ Evolution equation for sea surface height (η):   Using these boundary conditions, we obtain evolution equation for sea surface height η by vertically integrating the continuity equation (2.18),

$$\frac{\partial \eta}{\partial t} + \frac{1}{h_\mu h_\psi}\left\{\frac{\partial (h_\psi(H + \eta)\langle u \rangle)}{\partial \mu} + \frac{\partial (h_\mu(H + \eta)\langle v \rangle)}{\partial \psi}\right\} = P - E + R + I, \tag{2.29}$$

where $\langle (u, v) \rangle = \frac{1}{H+\eta} \int_{-H}^{\eta} (u, v) dz$.

d. Mixing at the surface boundary layer

Near the sea surface, strong vertical mixing may occur for stably stratified situations because of active turbulence. These processes occur on a small scale ($<$ several meters) and cannot be resolved in a large scale hydrostatic model with typical horizontal and vertical resolutions. These processes are parameterized as enhanced vertical viscosity and diffusivity. The user chooses whether to set a high vertical viscosity and diffusivity *a priori* or to use a surface boundary layer model. MRI.COM supports several surface boundary layer models. In the surface boundary layer models, vertical viscosity and diffusivity are calculated every time step. See Chapter 15 for details.

2.1.5   Generalized vertical coordinates

From MRI.COM version 4, the standard choice for the vertical coordinate is z^*, which was first introduced by Adcroft and Campin (2004). Before showing a specific expression of governing equations in z^* coordinate, we consider generalized vertical coordinates (s). Note that generalized vertical coordinates employed by ocean models are not orthogonal. Horizontal velocities are not perpendicular to the vertical coordinate but perpendicular to the local gravitational field. The generalized vertical coordinate surface $s = s(\mu, \psi, z, t)$ is expressed as a smooth function of the original coordinate and time. We introduce a new scale factor z_s, which measures the thickness in the original depth coordinate of the unit length in the new coordinate:

$$z_s \equiv \left.\frac{\partial z}{\partial s}\right|_{\mu\psi t}. \tag{2.30}$$

We further introduce vertical velocity $\dot{s}$ in generalized vertical coordinates.

Using a transformation rule presented by Adcroft and Campin (2004), we write the governing equations of the variables $(\mathbf{v}, \rho, \theta, S, p)$ in generalized vertical coordinates as follows:

$$\frac{\partial(z_s u)}{\partial t} + \frac{1}{h_\mu h_\psi} \left\{ \frac{\partial(z_s h_\psi u u)}{\partial \mu} + \frac{\partial(z_s h_\mu v u)}{\partial \psi} \right\} + \frac{\partial(z_s \dot{s} u)}{\partial s} + z_s \frac{v}{h_\mu h_\psi} \left(\frac{\partial h_\mu}{\partial \psi} u - \frac{\partial h_\psi}{\partial \mu} v \right) - z_s f v$$
$$= -z_s \frac{1}{\rho_0 h_\mu} \frac{\partial p}{\partial \mu} - z_s \frac{\rho}{\rho_0 h_\mu} \frac{\partial(gz)}{\partial \mu} + z_s \frac{1}{\rho_0} (\nabla \cdot \tau_{\text{horizontal strain}})_u + z_s \frac{1}{z_s} \frac{\partial}{\partial s} \left(\frac{\nu_V}{z_s} \frac{\partial u}{\partial s} \right), \quad (2.31)$$

$$\frac{\partial(z_s v)}{\partial t} + \frac{1}{h_\mu h_\psi} \left\{ \frac{\partial(z_s h_\psi u v)}{\partial \mu} + \frac{\partial(z_s h_\mu v v)}{\partial \psi} \right\} + \frac{\partial(z_s \dot{s} v)}{\partial s} + z_s \frac{u}{h_\mu h_\psi} \left(\frac{\partial h_\psi}{\partial \mu} v - \frac{\partial h_\mu}{\partial \psi} u \right) + z_s f u$$
$$= -z_s \frac{1}{\rho_0 h_\psi} \frac{\partial p}{\partial \psi} - z_s \frac{\rho}{\rho_0 h_\psi} \frac{\partial(gz)}{\partial \psi} + z_s \frac{1}{\rho_0} (\nabla \cdot \tau_{\text{horizontal strain}})_v + z_s \frac{1}{z_s} \frac{\partial}{\partial s} \left(\frac{\nu_V}{z_s} \frac{\partial v}{\partial s} \right), \quad (2.32)$$

$$\rho \frac{\partial(gz)}{\partial s} + \frac{\partial p}{\partial s} = 0, \quad (2.33)$$

$$\frac{\partial z_s}{\partial t} + \frac{1}{h_\mu h_\psi} \left\{ \frac{\partial(z_s h_\psi u)}{\partial \mu} + \frac{\partial(z_s h_\mu v)}{\partial \psi} \right\} + \frac{\partial(z_s \dot{s})}{\partial s} = 0, \quad (2.34)$$

$$\frac{\partial(z_s \theta)}{\partial t} + \frac{1}{h_\mu h_\psi} \left\{ \frac{\partial(z_s h_\psi u \theta)}{\partial \mu} + \frac{\partial(z_s h_\mu v \theta)}{\partial \psi} \right\} + \frac{\partial(z_s \dot{s} \theta)}{\partial s} = -z_s \nabla \cdot \mathbf{F}_\theta + z_s Q^\theta, \quad (2.35)$$

$$\frac{\partial(z_s S)}{\partial t} + \frac{1}{h_\mu h_\psi} \left\{ \frac{\partial(z_s h_\psi u S)}{\partial \mu} + \frac{\partial(z_s h_\mu v S)}{\partial \psi} \right\} + \frac{\partial(z_s \dot{s} S)}{\partial s} = -z_s \nabla \cdot \mathbf{F}_S + z_s Q^S, \quad (2.36)$$

and

$$\rho = \rho(\theta, S, p). \quad (2.37)$$

Evolution equation for sea surface height is obtained by vertically integrating the continuity equation (2.34) and considering the boundary condition. It has the same form as in the depth coordinate system:

$$\frac{\partial(\eta + H)}{\partial t} + \frac{1}{h_\mu h_\psi} \left[\frac{\partial(h_\psi U)}{\partial \mu} + \frac{\partial(h_\mu V)}{\partial \psi} \right] = P - E + R + I, \quad (2.38)$$

where

$$(U, V) = \int_{s(z=-H)}^{s(z=\eta)} [z_s(u, v)] ds. \quad (2.39)$$

2.1.6 z^* coordinate

a. Definition and boundary condition

Definition of the new vertical coordinate z^* is as follows:

$$z^* = \sigma(\mu, \psi, z, t) H(\mu, \psi) = \frac{z - \eta(\mu, \psi, t)}{H(\mu, \psi) + \eta(\mu, \psi, t)} H(\mu, \psi), \quad (2.40)$$

where $z = -H(\mu, \psi)$ is sea floor and η is the free surface displacement. σ is a symbol of the conventional terrain following vertical coordinate. In z^* coordinate, σ is further scaled by sea floor depth $H(\mu, \psi)$, which makes z^* coordinate more similar to the depth coordinate rather than the terrain following coordinate.

The scaling factor $z_s = \frac{\partial z}{\partial z^*}$ is

$$\frac{\partial z}{\partial z^*} = \frac{H + \eta}{H}. \quad (2.41)$$

The governing equations in z^* vertical coordinate are in the same form as equations (2.31) through (2.38), with z_s replaced by $z_{z^*} = \frac{H + \eta}{H}$.

The vertical velocity in this coordinate system is expressed as w^*, instead of $\dot{s}$. Here, w^* has the following relation with the vertical velocity w of the depth coordinate z,

$$w^* \equiv D_t z^* = \frac{H}{H + \eta} \left(w - \left(1 + \frac{z^*}{H} \right) D_t \eta + \frac{z^* \eta}{H^2} \mathbf{v}_h \cdot \nabla H \right), \quad (2.42)$$

where D_t represents the material time derivative operator in any coordinate system,

$$D_t \equiv \frac{\partial}{\partial t} + \mathbf{v} \cdot \nabla = \frac{\partial}{\partial t} + \frac{u}{h_\mu}\frac{\partial}{\partial \mu} + \frac{v}{h_\psi}\frac{\partial}{\partial \psi} + \frac{w}{z_s}\frac{\partial}{\partial s}. \tag{2.43}$$

Horizontal boundary conditions are unchanged by this coordinate transformation. Vertical boundary conditions need some discussion.

Sea floor ($z = -H$) in z^* coordinate is also $-H$.

$$z = -H(\mu, \psi) \implies z^* = -H(\mu, \psi). \tag{2.44}$$

Thus the kinematic boundary condition at sloping bottom is

$$w_{z=-H} = -\mathbf{v}_h \cdot \nabla H \implies w^*_{z^*=-H} = -\mathbf{v}_h \cdot \nabla H, \tag{2.45}$$

where $\mathbf{v}_h = (u, v, 0)$ is the horizontal component of velocity at $z = -H(\mu, \psi)$.

Sea surface ($z = \eta$) in z^* coordinate is

$$z = \eta(x, y, t) \implies z^* = 0. \tag{2.46}$$

Sea surface is fixed in time in z^* frame. In other words, model domain and grid cells are logically fixed in time. We do not have to concern about the moving sea surface and vanishing of the first layer thickness [§].

The kinematic boundary condition at the sea surface is

$$w_{z=\eta} = D_t\eta - (P - E + R + I) \implies w^*_{z^*=0} = -\frac{H}{H+\eta}(P - E + R + I). \tag{2.47}$$

For example, precipitation ($P > 0$) penetrates the ocean as a scaled downward vertical velocity.

b. Pressure gradient term

Horizontal momentum equations in generalized vertical coordinates (2.31), (2.32) involve both pressure gradient and geopotential gradient term. Pressure gradient error appears when these terms do not cancel each other. That said, pressure gradient error is not a big issue for z^* coordinate because horizontal gradient of a constant z^*-surface is usually very small. However, source of errors must be kept as small as possible. For this purpose, we first separate density into constant and its deviation

$$\rho = \rho_0 + \rho'(x, y, z^*, t). \tag{2.48}$$

Pressure is also separated in the same manner ($p = p_0 + p'$) and the hydrostatic relation (2.33) is separated into two equations

$$\partial_{z^*} p_0 = -g\left(\frac{H+\eta}{H}\right)\rho_0 \text{ and } p_0(z^* = 0) = 0, \tag{2.49}$$

$$\partial_{z^*} p' = -g\left(\frac{H+\eta}{H}\right)\rho' \text{ and } p'(z^* = 0) = p_a, \tag{2.50}$$

where p_a is atmospheric pressure[¶]. Specific expression for p_0 is obtained by integrating (2.49)

$$p_0(z^*) = p_0(x, y, z, t) = -g\rho_0\frac{H+\eta}{H}z^* = g\rho_0(\eta - z) = g\rho_0\eta - \rho_0\Phi. \tag{2.51}$$

Rewriting pressure gradient term by using this, we have

$$\frac{1}{\rho_0}\nabla_{z^*}(p_0 + p') + \frac{\rho}{\rho_0}\nabla_{z^*}\Phi = g\nabla\eta - \nabla_{z^*}\Phi + \frac{1}{\rho_0}\nabla_{z^*}p' + \frac{\rho_0 + \rho'}{\rho_0}\nabla_{z^*}\Phi \tag{2.52}$$

$$= g\nabla\eta + \frac{1}{\rho_0}\nabla_{z^*}p' + \frac{\rho'}{\rho_0}\nabla_{z^*}\Phi. \tag{2.53}$$

[§] However, sea surface is not allowed to touch the see floor ($H + \eta \leq 0$), which is a local problem. This is a restrictive condition inherent to this coordinate system.

[¶] Ice-loading effect (e.g., Campin et al., 2008) has not been included in MRI.COM

It is noticed that time-independent terms are removed. Because geopotential is $\Phi = gz$, the momentum equation is expressed as

$$\partial_t \mathbf{v}_h + \mathbf{v}_h \cdot \nabla_{z^*} \mathbf{v}_h + w^* \partial_{z^*} \mathbf{v}_h + f\hat{\mathbf{z}} \times \mathbf{v}_h + g\nabla\eta + \frac{1}{\rho_0} \nabla_{z^*} p' + \frac{g\rho'}{\rho_0} \nabla_{z^*} z = \mathbf{F} \tag{2.54}$$

Perturbation pressure is obtained by integrating (2.50) as

$$p'(z^*) = p_a + g \int_{z^*}^0 \rho' z_{z^*} dz^* = p_a + g \int_{z(z^*)}^{\eta} \rho' dz. \tag{2.55}$$

Then (2.54) becomes

$$\partial_t \mathbf{v}_h + \mathbf{v}_h \cdot \nabla_{z^*} \mathbf{v}_h + w^* \partial_{z^*} \mathbf{v}_h + f\hat{\mathbf{z}} \times \mathbf{v}_h$$
$$+ \underbrace{\frac{1}{\rho_0} \nabla_{z^*} (p_a + g\rho_0\eta)}_{\text{fast}} + \underbrace{\frac{1}{\rho_0} \nabla_{z^*} \left(g \int_{z(z^*)}^{\eta} \rho' dz \right) + \frac{g\rho'}{\rho_0} \nabla_{z^*} z}_{\text{slow}} = \mathbf{F}. \tag{2.56}$$

We separate the pressure gradient term into barotropic (fast) and baroclinic (slow) component in preparation for the split-explicit solution method for equations of motion.

2.2   Numerical Methods

2.2.1   Discretization and finite volume method

To solve the primitive equations formulated in the previous section, the equations are projected on a discrete lattice and then advanced for a discrete time interval.

Because primary choice of the vertical coordinate of MRI.COM is z^*, a logically fixed (but actually moving) Eulerian lattice is arranged. A detailed description of the grid arrangement is given in Chapter 3. The equations are then volume integrated over a discrete model grid cell. This approach is called a finite volume approach or sometimes a flux form expression in this manual.

A vertically integrated expression for the primitive equations is useful for describing the solution procedure. These are called semi-discrete equations (Griffies, 2004). The body force and metric terms will be simply multiplied by the grid width. The material transport and subgrid-scale flux terms need some attention.

In this section the vertical coordinate of z^* is written as a general symbol s. The material transport of any quantity α that commonly appears in the prognostic equations,

$$\frac{\partial(z_s \alpha)}{\partial t} + \frac{1}{h_\mu h_\psi} \left\{ \frac{\partial(h_\psi z_s u\alpha)}{\partial \mu} + \frac{\partial(h_\mu z_s v\alpha)}{\partial \psi} \right\} + \frac{\partial(z_s \dot{s}\alpha)}{\partial s} \tag{2.57}$$

is vertically integrated over a $(k - \frac{1}{2})$-th grid cell bounded by s_{k-1} and s_k to give

$$\int_{s_k}^{s_{k-1}} \frac{\partial(z_s\alpha)}{\partial t} ds + \int_{s_k}^{s_{k-1}} \frac{1}{h_\mu h_\psi} \left\{ \frac{\partial(h_\psi z_s u\alpha)}{\partial \mu} + \frac{\partial(h_\mu z_s v\alpha)}{\partial \psi} \right\} ds + \int_{s_k}^{s_{k-1}} \frac{\partial(z_s \dot{s}\alpha)}{\partial s} ds$$
$$= \frac{\partial}{\partial t} \left(\int_{s_k}^{s_{k-1}} (z_s\alpha) ds \right) + \frac{1}{h_\mu h_\psi} \left\{ \frac{\partial}{\partial \mu} \left(\int_{s_k}^{s_{k-1}} h_\psi z_s u\alpha \, ds \right) + \frac{\partial}{\partial \psi} \left(\int_{s_k}^{s_{k-1}} h_\mu z_s v\alpha \, ds \right) \right\}$$
$$- \left(z_s \frac{\partial s_{k-1}}{\partial t} + \frac{z_s u(s_{k-1})}{h_\mu} \frac{\partial s_{k-1}}{\partial \mu} + \frac{z_s v(s_{k-1})}{h_\psi} \frac{\partial s_{k-1}}{\partial \psi} - z_s \dot{s}(s_{k-1}) \right) \alpha(s_{k-1})$$
$$+ \left(z_s \frac{\partial s_k}{\partial t} + \frac{z_s u(s_k)}{h_\mu} \frac{\partial s_k}{\partial \mu} + \frac{z_s v(s_k)}{h_\psi} \frac{\partial s_k}{\partial \psi} - z_s \dot{s}(s_k) \right) \alpha(s_k). \tag{2.58}$$

The first line on the r.h.s. is expressed in a semi-discrete form as

$$\frac{\partial}{\partial t} \left(\Delta z\alpha \right)_{k-\frac{1}{2}} + \frac{1}{h_\mu h_\psi} \left\{ \frac{\partial}{\partial \mu} \left(h_\psi \Delta z u\alpha \right)_{k-\frac{1}{2}} + \frac{\partial}{\partial \psi} \left(h_\mu \Delta z v\alpha \right)_{k-\frac{1}{2}} \right\}, \tag{2.59}$$

where any quantity is assumed to have a uniform distribution within a grid cell.

Using $\dot{s} \equiv D_t s$ and (2.43), the last two lines are reduced to the difference between vertical advective fluxes:

$$\text{the last two lines of (2.58)} = z_s \dot{s}(s_{k-1})\alpha(s_{k-1}) - z_s \dot{s}(s_k)\alpha(s_k). \tag{2.60}$$

For the sea surface ($k = 1$; $s_0 = 0$) and the bottom ($k = kbtm$; $s_{kbtm} = -H$), kinematic conditions (2.47) and (2.45) are used to give

$$\text{the last two lines of (2.58)} = -(P - E + R + I)\alpha(0) - z_s \dot{s}(s_1)\alpha(s_1) \tag{2.61}$$

at the surface and

$$\text{the last two lines of (2.58)} = z_s \dot{s}(s_{kbtm-1})\alpha(s_{kbtm-1}) - 0 \tag{2.62}$$

at the bottom (bottom term vanishes to give no advective fluxes through the sea floor).

Similarly, the vertical integral of the divergence of the subgrid-scale fluxes gives

$$\int_{s_k}^{s_{k-1}} \frac{1}{h_\mu h_\psi} \left\{ \frac{\partial(h_\psi z_s F_\mu)}{\partial\mu} + \frac{\partial(h_\mu z_s F_\psi)}{\partial\psi} \right\} ds + \int_{s_k}^{s_{k-1}} \frac{\partial F_s}{\partial s} ds$$
$$= \frac{1}{h_\mu h_\psi} \left\{ \frac{\partial}{\partial\mu}\left(h_\psi \Delta z F_\mu\right)_{k-\frac{1}{2}} + \frac{\partial}{\partial\psi}\left(h_\mu \Delta z F_\psi\right)_{k-\frac{1}{2}} \right\}$$
$$- \left(\frac{F_\mu(s)}{h_\mu}\frac{\partial s}{\partial\mu} + \frac{F_\psi(s)}{h_\psi}\frac{\partial s}{\partial\psi} - F_s(s) \right)_{k-1} + \left(\frac{F_\mu(s)}{h_\mu}\frac{\partial s}{\partial\mu} + \frac{F_\psi(s)}{h_\psi}\frac{\partial s}{\partial\psi} - F_s(s) \right)_k. \tag{2.63}$$

In summary, the material transport and subgrid-scale flux parts are integrated for a vertical grid cell to give the semi-discrete expression on the r.h.s.,

$$\int_{s_k}^{s_{k-1}} \frac{\partial(z_s \alpha)}{\partial t} ds + \int_{s_k}^{s_{k-1}} \frac{1}{h_\mu h_\psi} \left\{ \frac{\partial(h_\psi z_s u\alpha)}{\partial\mu} + \frac{\partial(h_\mu z_s v\alpha)}{\partial\psi} \right\} ds + \int_{s_k}^{s_{k-1}} \frac{\partial(z_s \dot{s}\alpha)}{\partial s} ds$$
$$+ \int_{s_k}^{s_{k-1}} \frac{1}{h_\mu h_\psi} \left\{ \frac{\partial(h_\psi z_s F_\mu)}{\partial\mu} + \frac{\partial(h_\mu z_s F_\psi)}{\partial\psi} \right\} ds + \int_{s_k}^{s_{k-1}} \frac{\partial F_s}{\partial s} ds$$
$$= \frac{\partial}{\partial t}\left(\Delta z \alpha\right)_{k-\frac{1}{2}} + \frac{1}{h_\mu h_\psi} \left\{ \frac{\partial}{\partial\mu}\left(h_\psi \Delta z u\alpha\right)_{k-\frac{1}{2}} + \frac{\partial}{\partial\psi}\left(h_\mu \Delta z v\alpha\right)_{k-\frac{1}{2}} \right\} + z_s \dot{s}(s_{k-1})\alpha(s_{k-1}) - z_s \dot{s}(s_k)\alpha(s_k)$$
$$+ \frac{1}{h_\mu h_\psi} \left\{ \frac{\partial}{\partial\mu}\left(h_\psi \Delta z F_\mu\right)_{k-\frac{1}{2}} + \frac{\partial}{\partial\psi}\left(h_\mu \Delta z F_\psi\right)_{k-\frac{1}{2}} \right\} + F_s(s_{k-1}) - F_s(s_k). \tag{2.64}$$

The quantity

$$F_{\text{surf}}^{\alpha} = (P - E + R + I)\alpha(0) + \left(\frac{F_\mu(s_0)}{h_\mu}\frac{\partial s_0}{\partial\mu} + \frac{F_\psi(s_0)}{h_\psi}\frac{\partial s_0}{\partial\psi} - F_s(s_0) \right) = (P - E + R + I)\alpha(0) - F_s(0) \tag{2.65}$$

taken from (2.61) and (2.63) may be regarded as a surface forcing term and corresponds to the surface flux (positive downward) given in the previous section. The first term on the r.h.s. of (2.65) is the tracer transport by the fresh water flux, and the second term is the microstructure flux calculated by subgrid-scale parameterizations such as bulk formula. Similarly, geothermal heating may be incorporated as microstructure flux from the sea floor ($\mathbf{F}_h(-H) \cdot \nabla_h H + F_s(-H)$).

2.2.2   Mode splitting in the momentum equation

Here we consider to solve the momentum equation with hydrostatic and Boussinesq approximation. Equations are (2.31), (2.32), and (2.33). To integrate these equations in time, we should know the instantaneous vector field, pressure, and geopotential. For the vector field, we use one at the previous time level. We obtain the pressure field by integrating the hydrostatic equation vertically, in which the sea surface height ($z = \eta$) is needed. The sea surface height is also needed for geopotential. To obtain the surface height, we should solve vertically integrated continuity equation (2.38).

The rise and fall of the sea level causes external gravity waves whose phase speed is two orders of magnitude greater than that of other waves. This will impose tight limits on the time intervals due to the CFL condition. We want to separate or remove external gravity waves, because they are usually not important when a target phenomenon has a longer time scale.

Historically, external gravity waves were removed from the model by prohibiting the vertical movement of the sea surface (rigid-lid approximation). In this case, the vertically integrated equations result in a vorticity equation in the form of the Poisson equation, solved by relaxation methods. The surface pressure is then diagnostically obtained as the pressure pushing up the lid.

After the sea surface was allowed to move vertically, the problem of fast external modes was resolved by separating the barotropic mode from the baroclinic mode. The barotropic mode is solved explicitly with a short time step. The baroclinic mode can take a longer time step by reflecting a state of the barotropic mode in which high-frequency components are

filtered out. Since this free surface option is more suitable for parallel computation than the rigid-lid approximation, only the free surface option is supported by MRI.COM. The essence of the split-explicit free surface formulation is explained below. See Chapter 7 for details.

a. Barotropic mode

Following (2.39), if we put

$$U = \int_{-H}^{0} z_s u \, ds = \sum_{k=1}^{N} u_{k-\frac{1}{2}} \Delta z_{k-\frac{1}{2}}, \quad V = \int_{-H}^{0} z_s v \, ds = \sum_{k=1}^{N} v_{k-\frac{1}{2}} \Delta z_{k-\frac{1}{2}}, \tag{2.66}$$

and separate fast and slow modes of the pressure gradient as in (2.56), then the vertically summed semi-discrete momentum equations are

$$\frac{\partial U}{\partial t} - fV = -\frac{(\eta + H)}{\rho_0 h_\mu} \frac{\partial (p_a + g\rho_0 \eta)}{\partial \mu} + X, \tag{2.67}$$

$$\frac{\partial V}{\partial t} + fU = -\frac{(\eta + H)}{\rho_0 h_\psi} \frac{\partial (p_a + g\rho_0 \eta)}{\partial \psi} + Y, \tag{2.68}$$

where p_a is the atmospheric pressure at sea surface. Density ρ has been separated into mean ρ_0 and perturbation ρ', and

$$
X = -\nabla_H \cdot \Big(\sum_{k=1}^{N} (\Delta z(u, \ v)u)_{k-\frac{1}{2}} \Big) - \sum_{k=1}^{N} \Big[\frac{v}{h_\mu h_\psi} \Big(\frac{\partial h_\mu}{\partial \psi} u - \frac{\partial h_\psi}{\partial \mu} v \Big) \Big]_{k-\frac{1}{2}} \Delta z_{k-\frac{1}{2}}
$$

$$
- \sum_{k=1}^{N} \Big[\frac{1}{\rho_0} \frac{1}{h_\mu} \int_{s_{k-\frac{1}{2}}}^{0} z_s g \rho_\mu \, ds' \Big] \Delta z_{k-\frac{1}{2}} - \frac{g}{\rho_0 h_\mu} \sum_{k=1}^{N} [\rho' z_\mu] \Delta z_{k-\frac{1}{2}} + \sum_{k=1}^{N} (\Delta z F_{\text{horz}}^\mu)_{k-\frac{1}{2}} + F_{\text{surf}}^\mu \Delta z_{\frac{1}{2}} + F_{\text{bottom}}^\mu \Delta z_{N-\frac{1}{2}}
$$

$$
(\equiv \sum_{k=1}^{N} F_\mu), \tag{2.69}
$$

$$
Y = -\nabla_H \cdot \Big(\sum_{k=1}^{N} (\Delta z(u, \ v)v)_{k-\frac{1}{2}} \Big) + \sum_{k=1}^{N} \Big[\frac{u}{h_\mu h_\psi} \Big(\frac{\partial h_\mu}{\partial \psi} u - \frac{\partial h_\psi}{\partial \mu} v \Big) \Big]_{k-\frac{1}{2}} \Delta z_{k-\frac{1}{2}}
$$

$$
- \sum_{k=1}^{N} \Big[\frac{1}{\rho_0} \frac{1}{h_\psi} \int_{s_{k-\frac{1}{2}}}^{0} z_s g \rho_\psi \, ds' \Big] \Delta z_{k-\frac{1}{2}} - \frac{g}{\rho_0 h_\psi} \sum_{k=1}^{N} [\rho' z_\psi] \Delta z_{k-\frac{1}{2}} + \sum_{k=1}^{N} (\Delta z F_{\text{horz}}^\psi)_{k-\frac{1}{2}} + F_{\text{surf}}^\psi \Delta z_{\frac{1}{2}} + F_{\text{bottom}}^\psi \Delta z_{N-\frac{1}{2}}
$$

$$
(\equiv \sum_{k=1}^{N} F_\psi). \tag{2.70}
$$

The vertically integrated continuity equation is given by

$$\frac{\partial \eta}{\partial t} + \frac{1}{h_\mu h_\psi} \Big(\frac{\partial (h_\psi U)}{\partial \mu} + \frac{\partial (h_\mu V)}{\partial \psi} \Big) = (P - E + R + I). \tag{2.71}$$

We solve these equations for U, V, and η with a short time step constrained by the phase speed of the external gravity waves.

On returning (U, V) to the baroclinic mode, the effect of high-frequency phenomena with time scale shorter than the baroclinic time step is filtered out by a weighted averaging, which is symbolically expressed as follows:

$$\langle U \rangle^{n+1} = U^n + \Delta t_{\text{cl}} f \langle\langle V \rangle\rangle^{n+\frac{1}{2}} - \Delta t_{\text{cl}} \Big\langle \Big\langle \frac{(\eta + H)}{\rho_0 h_\mu} \frac{\partial (p_a + \rho_0 g \eta)}{\partial \mu} \Big\rangle \Big\rangle^{n+\frac{1}{2}} + \Delta t_{\text{cl}} X^n, \tag{2.72}$$

$$\langle V \rangle^{n+1} = V^n - \Delta t_{\text{cl}} f \langle\langle U \rangle\rangle^{n+\frac{1}{2}} - \Delta t_{\text{cl}} \Big\langle \Big\langle \frac{(\eta + H)}{\rho_0 h_\psi} \frac{\partial (p_a + \rho_0 g \eta)}{\partial \psi} \Big\rangle \Big\rangle^{n+\frac{1}{2}} + \Delta t_{\text{cl}} Y^n, \tag{2.73}$$

where $\langle \cdot \rangle^{n+1} \equiv \sum_{m=1}^{M^*} b_m (\cdot)^{m-\frac{1}{2}}$ and $\langle\langle \cdot \rangle\rangle^{n+\frac{1}{2}} \equiv \sum_{m=1}^{M^*} b_m \sum_{m'=1}^{m} (\cdot)^{m'-\frac{1}{2}}$, with $m \in \{1, M^*\}$ representing the barotropic time level, n representing the baroclinic time level, Δt_{cl} being the baroclinic time step, and b_m being weighting factors explained in Chapter 7. The above equations are used to obtain absolute velocity with equations of the baroclinic mode described in this subsection (see below). See Sec. (7.7) for detais of the formulation.

b. Baroclinic mode

Velocity is decomposed into a barotropic component based on (2.39), $(\bar{u}, \bar{v})$, and a baroclinic component, $(\hat{u}, \hat{v})$, as follows:

$$u = \hat{u} + \bar{u}, \qquad v = \hat{v} + \bar{v}, \tag{2.74}$$

where

$$\bar{u} = \frac{1}{H}U, \qquad \bar{v} = \frac{1}{H}V. \tag{2.75}$$

By solving the baroclinc mode $(\hat{u}, \hat{v})$, absolute velocity (u, v) at the next step is obtained.

First, we drop the fast pressure gradient term from the momentum equation, (2.31) and (2.32), since it is a barotropic component:

$$
\frac{\partial(z_s u)}{\partial t} + \frac{1}{h_\mu h_\psi} \left\{ \frac{\partial(z_s h_\psi uu)}{\partial \mu} + \frac{\partial(z_s h_\mu vu)}{\partial \psi} \right\} + \frac{\partial(z_s \dot{s} u)}{\partial s} + z_s \frac{v}{h_\mu h_\psi} \left(\frac{\partial h_\mu}{\partial \psi} u - \frac{\partial h_\psi}{\partial \mu} v \right) - z_s f v
$$
$$
= -z_s \frac{1}{\rho_0 h_\mu} \frac{\partial}{\partial \mu} \left(g \int_{z(z^*)}^{\eta} \rho' dz \right) - z_s \frac{g\rho'}{\rho_0 h_\mu} \frac{\partial z}{\partial \mu}
$$
$$
+ z_s \frac{1}{\rho_0} (\nabla \cdot \tau_{\text{horizontal strain}})_u + z_s \frac{1}{z_s} \frac{\partial}{\partial s} \left(\frac{\nu_V}{z_s} \frac{\partial u}{\partial s} \right), \tag{2.76}
$$

$$
\frac{\partial(z_s v)}{\partial t} + \frac{1}{h_\mu h_\psi} \left\{ \frac{\partial(z_s h_\psi uv)}{\partial \mu} + \frac{\partial(z_s h_\mu vv)}{\partial \psi} \right\} + \frac{\partial(z_s \dot{s} v)}{\partial s} + z_s \frac{u}{h_\mu h_\psi} \left(\frac{\partial h_\psi}{\partial \mu} v - \frac{\partial h_\mu}{\partial \psi} u \right) + z_s f u
$$
$$
= -z_s \frac{1}{\rho_0 h_\psi} \frac{\partial}{\partial \psi} \left(g \int_{z(z^*)}^{\eta} \rho' dz \right) - z_s \frac{g\rho'}{\rho_0 h_\psi} \frac{\partial z}{\partial \psi}
$$
$$
+ z_s \frac{1}{\rho_0} (\nabla \cdot \tau_{\text{horizontal strain}})_v, + z_s \frac{1}{z_s} \frac{\partial}{\partial s} \left(\frac{\nu_V}{z_s} \frac{\partial v}{\partial s} \right). \tag{2.77}
$$

Using these equations, provisional velocity (u', v') at the next step is calculated. In discrete forms,

$$
\frac{u'_{k-\frac{1}{2}} \Delta z^{n+1}_{k-\frac{1}{2}} - u^n_{k-\frac{1}{2}} \Delta z^n_{k-\frac{1}{2}}}{\Delta t_{\text{cl}}} = f[v_{k-\frac{1}{2}} \Delta z_{k-\frac{1}{2}}]^{n+\frac{1}{2}} + F^n_\mu, \tag{2.78}
$$

$$
\frac{v'_{k-\frac{1}{2}} \Delta z^{n+1}_{k-\frac{1}{2}} - v^n_{k-\frac{1}{2}} \Delta z^n_{k-\frac{1}{2}}}{\Delta t_{\text{cl}}} = -f[u_{k-\frac{1}{2}} \Delta z_{k-\frac{1}{2}}]^{n+\frac{1}{2}} + F^n_\psi, \tag{2.79}
$$

where

$$
F^n_\mu = -\nabla_H \cdot \left(\Delta z(u, \ v)u \right)_{k-\frac{1}{2}} - \left[\frac{v}{h_\mu h_\psi} \left(\frac{\partial h_\mu}{\partial \psi} u - \frac{\partial h_\psi}{\partial \mu} v \right) \right]_{k-\frac{1}{2}} \Delta z_{k-\frac{1}{2}}
$$
$$
- \left[\frac{1}{\rho_0} \frac{1}{h_\mu} \int_{s_{k-\frac{1}{2}}}^0 z_s g \rho_\mu ds' \right] \Delta z_{k-\frac{1}{2}} - \frac{g}{\rho_0 h_\mu} \sum_{k=1}^{N} [\rho' z_\mu] \Delta z_{k-\frac{1}{2}} + (\Delta z F^\mu_{\text{horz}})_{k-\frac{1}{2}} - F^\mu_{\text{vert}\,k-1} + F^\mu_{\text{vert}\,k}, \tag{2.80}
$$

$$
F^n_\psi = -\nabla_H \cdot \left(\Delta z(u, \ v)v \right)_{k-\frac{1}{2}} + \left[\frac{u}{h_\mu h_\psi} \left(\frac{\partial h_\mu}{\partial \psi} u - \frac{\partial h_\psi}{\partial \mu} v \right) \right]_{k-\frac{1}{2}} \Delta z_{k-\frac{1}{2}}
$$
$$
- \left[\frac{1}{\rho_0} \frac{1}{h_\psi} \int_{s_{k-\frac{1}{2}}}^0 z_s g \rho_\psi ds' \right] \Delta z_{k-\frac{1}{2}} - \frac{g}{\rho_0 h_\psi} \sum_{k=1}^{N} [\rho' z_\psi] \Delta z_{k-\frac{1}{2}} + (\Delta z F^\psi_{\text{horz}})_{k-\frac{1}{2}} - F^\psi_{\text{vert}\,k-1} + F^\psi_{\text{vert}\,k}. \tag{2.81}
$$

A method for solving these equations is explained in Chapter 8.

Next, using (u', v'), baroclinic component $(\hat{u}, \hat{v})$ and absolute velocity (u, v) at the next step are calculated. Summing over the whole water column gives

$$
\frac{\sum_{k=1}^{N} (u'_{k-\frac{1}{2}} \Delta z^{n+1}_{k-\frac{1}{2}}) - \sum_{k=1}^{N} (u^n_{k-\frac{1}{2}} \Delta z^n_{k-\frac{1}{2}})}{\Delta t_{\text{cl}}} = f \sum_{k=1}^{N} [v_{k-\frac{1}{2}} \Delta z_{k-\frac{1}{2}}]^{n+\frac{1}{2}} + X^n, \tag{2.82}
$$

$$
\frac{\sum_{k=1}^{N} (v'_{k-\frac{1}{2}} \Delta z^{n+1}_{k-\frac{1}{2}}) - \sum_{k=1}^{N} (v^n_{k-\frac{1}{2}} \Delta z^n_{k-\frac{1}{2}})}{\Delta t_{\text{cl}}} = -f \sum_{k=1}^{N} [u_{k-\frac{1}{2}} \Delta z_{k-\frac{1}{2}}]^{n+\frac{1}{2}} + Y^n. \tag{2.83}
$$

X^n and Y^n are removed by using the equations from the barotropic mode (2.72), (2.73) to give

$$\frac{\sum_{k=1}^{N}(\langle u\rangle^{n+1}\Delta z_{k-\frac{1}{2}}^{n+1}) - \sum_{k=1}^{N}(u'_{k-\frac{1}{2}}\Delta z_{k-\frac{1}{2}}^{n+1})}{\Delta t_{\text{cl}}} = f\langle\langle V\rangle\rangle^{n+\frac{1}{2}} - f\sum_{k=1}^{N}[v_{k-\frac{1}{2}}\Delta z_{k-\frac{1}{2}}]^{n+\frac{1}{2}} - \left\langle\left\langle\frac{(\eta+H)}{\rho_0 h_\mu}\frac{\partial(p_a+\rho_0 g\eta)}{\partial\mu}\right\rangle\right\rangle^{n+\frac{1}{2}},$$
(2.84)

$$\frac{\sum_{k=1}^{N}(\langle v\rangle^{n+1}\Delta z_{k-\frac{1}{2}}^{n+1}) - \sum_{k=1}^{N}(v'_{k-\frac{1}{2}}\Delta z_{k-\frac{1}{2}}^{n+1})}{\Delta t_{\text{cl}}} = -f\langle\langle U\rangle\rangle^{n+\frac{1}{2}} + f\sum_{k=1}^{N}[u_{k-\frac{1}{2}}\Delta z_{k-\frac{1}{2}}]^{n+\frac{1}{2}} - \left\langle\left\langle\frac{(\eta+H)}{\rho_0 h_\psi}\frac{\partial(p_a+\rho_0 g\eta)}{\partial\psi}\right\rangle\right\rangle^{n+\frac{1}{2}}.$$
(2.85)

where $\langle u\rangle^{n+1} = \langle U\rangle^{n+1}/(\eta^{n+1}+H)$ and $\langle v\rangle^{n+1} = \langle V\rangle^{n+1}/(\eta^{n+1}+H)$. This is combined with (2.78) and (2.79) to give

$$\frac{\left(u'_{k-\frac{1}{2}} - \overline{u'}^z + \langle u\rangle^{n+1}\right)\Delta z_{k-\frac{1}{2}}^{n+1} - u_{k-\frac{1}{2}}^n\Delta z_{k-\frac{1}{2}}^n}{\Delta t_{\text{cl}}} = f\left[v_{k-\frac{1}{2}}\Delta z_{k-\frac{1}{2}}\right]^{n+\frac{1}{2}} - f\overline{[v]^{n+\frac{1}{2}}}^z\Delta z_{k-\frac{1}{2}}^{n+1} + f\langle\langle v\rangle\rangle^{n+\frac{1}{2}}\Delta z_{k-\frac{1}{2}}^{n+1}$$
$$- \frac{\Delta z_{k-\frac{1}{2}}^{n+1}}{\eta^{n+1}+H}\left\langle\left\langle\frac{(\eta+H)}{\rho_0 h_\mu}\frac{\partial(p_a+\rho_0 g\eta)}{\partial\mu}\right\rangle\right\rangle^{n+\frac{1}{2}} + F_\mu^n$$
(2.86)

$$\frac{\left(v'_{k-\frac{1}{2}} - \overline{v'}^z + \langle v\rangle^{n+1}\right)\Delta z_{k-\frac{1}{2}}^{n+1} - v_{k-\frac{1}{2}}^n\Delta z_{k-\frac{1}{2}}^n}{\Delta t_{\text{cl}}} = -f\left[u_{k-\frac{1}{2}}\Delta z_{k-\frac{1}{2}}\right]^{n+\frac{1}{2}} + f\overline{[u]^{n+\frac{1}{2}}}^z\Delta z_{k-\frac{1}{2}}^{n+1} - f\langle\langle u\rangle\rangle^{n+\frac{1}{2}}\Delta z_{k-\frac{1}{2}}^{n+1}$$
$$- \frac{\Delta z_{k-\frac{1}{2}}^{n+1}}{\eta^{n+1}+H}\left\langle\left\langle\frac{(\eta+H)}{\rho_0 h_\psi}\frac{\partial(p_a+\rho_0 g\eta)}{\partial\psi}\right\rangle\right\rangle^{n+\frac{1}{2}} + F_\psi^n,$$
(2.87)

where $\overline{(...)}^z$ denotes the thickness weighted vertical average.

Since $f\overline{[v]^{n+\frac{1}{2}}}^z\Delta z_{k-\frac{1}{2}}^{n+1} \sim f\langle\langle v\rangle\rangle^{n+\frac{1}{2}}\Delta z_{k-\frac{1}{2}}^{n+1}$, $f\overline{[u]^{n+\frac{1}{2}}}^z\Delta z_{k-\frac{1}{2}}^{n+1} \sim f\langle\langle u\rangle\rangle^{n+\frac{1}{2}}\Delta z_{k-\frac{1}{2}}^{n+1}$, and the fourth terms on the r. h. s. are the surface pressure gradient, we may regard $u' - \overline{u'}^z + \langle u\rangle^{n+1}$ and $v' - \overline{v'}^z + \langle v\rangle^{n+1}$ as the real updated velocity for time level $n+1$, the baroclinic component is expressed as $\hat{u} = u' - \overline{u'}$ and $\hat{v} = v' - \overline{v'}$.

To summarize, we first solve for (u',v') using (2.78) and (2.79), and then compute the baroclinic component by $\hat{u} = u' - \overline{u'}$ and $\hat{v} = v' - \overline{v'}$. The absolute velocity is obtained by $u = \hat{u} + \bar{u}$ and $v = \hat{v} + \bar{v}$.

2.3 Appendix

2.3.1 Acceleration method

It usually takes several thousand years before the global thermohaline circulation reaches a steady state under (quasi-)steady forcing. The limiting factor for the time step is the phase speed of external gravity waves ($\sim 200\,\text{m/s}$) for the barotropic mode and that of internal gravity waves ($\sim$ a few m/s) for the baroclinic mode. A several-thousand-year integration will not be a workable exercise as long as we are restricted by this criterion in determining the time step. Bryan (1984) proposed a method to accelerate the ocean's convergence to equilibrium. In this method, the phase speed of waves is reduced by modifying the governing equations, and a thermally balanced state is quickly reached by reducing the specific heat.

Specifically, they are achieved by multiplying a constant to the tendency terms (α for momentum and γ for tracers) to increase inertia and to reduce specific heat. When a steady state is reached in these equations, we expect that the same balance as the undistorted equations will be obtained, because the only difference between the distorted and undistorted equations are tendency terms, which are expected to be zero in the steady state.

The modified momentum equation is given by

$$\alpha\frac{\partial u}{\partial t} + \frac{1}{h_\mu h_\psi}\left\{\frac{\partial(h_\psi uu)}{\partial\mu} + \frac{\partial(h_\mu vu)}{\partial\psi}\right\} + \frac{\partial(wu)}{\partial z} + \frac{v}{h_\mu h_\psi}\left(\frac{\partial h_\mu}{\partial\psi}u - \frac{\partial h_\psi}{\partial\mu}v\right) - fv$$
$$= -\frac{1}{\rho_0 h_\mu}\frac{\partial p}{\partial\mu} + \frac{1}{\rho_0}(\nabla\cdot\tau_{\text{horizontal strain}})_u + \frac{\partial}{\partial z}\left(\nu_V\frac{\partial u}{\partial z}\right),$$
(2.88)

$$\alpha\frac{\partial v}{\partial t} + \frac{1}{h_\mu h_\psi}\left\{\frac{\partial(h_\psi uv)}{\partial\mu} + \frac{\partial(h_\mu vv)}{\partial\psi}\right\} + \frac{\partial(wv)}{\partial z} + \frac{u}{h_\mu h_\psi}\left(\frac{\partial h_\psi}{\partial\mu}v - \frac{\partial h_\mu}{\partial\psi}u\right) + fu$$
$$= -\frac{1}{\rho_0 h_\psi}\frac{\partial p}{\partial\psi} + \frac{1}{\rho_0}(\nabla\cdot\tau_{\text{horizontal strain}})_v + \frac{\partial}{\partial z}\left(\nu_V\frac{\partial v}{\partial z}\right).$$
(2.89)

The modified temperature and salinity equations are given by

$$\gamma \frac{\partial \theta}{\partial t} = -\frac{1}{h_\mu h_\psi} \left\{ \frac{\partial (h_\psi u\theta)}{\partial \mu} + \frac{\partial (h_\mu v\theta)}{\partial \psi} \right\} - \frac{\partial (w\theta)}{\partial z} - \nabla \cdot \mathbf{F}^\theta + Q^\theta, \tag{2.90}$$

$$\gamma \frac{\partial S}{\partial t} = -\frac{1}{h_\mu h_\psi} \left\{ \frac{\partial (h_\psi uS)}{\partial \mu} + \frac{\partial (h_\mu vS)}{\partial \psi} \right\} - \frac{\partial (wS)}{\partial z} - \nabla \cdot \mathbf{F}^S + Q^S. \tag{2.91}$$

Here, equations are written in depth (z) coordinate for brevity.

These modifications are equivalent to changing time to $t' = t/\alpha$ and the Brunt-Vaisala frequency to $N'^2 = N^2 \alpha / \gamma$. In this case, the equivalent depth for the n-th mode of the vertical mode decomposition becomes $H'_n = H_n / \alpha$.

The dispersion relation for the free inertia-gravity waves becomes:

$$\omega^2 = \frac{f^2}{\alpha^2} + \left(\frac{gH_n}{\alpha} \right)(k^2 + l^2). \tag{2.92}$$

Since the angular frequency ω is inversely proportional to $\alpha^{1/2}$, the phase speed becomes low for large α. The model can be run with a long time step.

The dispersion relation for Rossby waves becomes:

$$\omega = -\beta k \left[\alpha (k^2 + l^2) + \frac{f^2}{gH_n} \right]^{-1}. \tag{2.93}$$

Again, a large α yields a low phase speed.

In standard practice, a value from several tens to a few hundred is used as α, a value of one is used near the sea surface, and a value about a tenth is used near the bottom as γ.

It should be noted that when α is too large, the model field is prone to baroclinic instability. Since this should not occur in nature, an integration of the model should be performed carefully by checking outputs during the integration.

2.3.2   Physical constants

On Table 2.1, we list basic physical constants used for MRI.COM. These are defined in `param.F90`. Physical constants or formulae used to calculate surface fluxes and sea ice processes are explained in Chapters 14 and 17, respectively.

<div align="center">Table2.1   Physical constants used in the model</div>

	value	variable name in MRI.COM
radius of the Earth	6375.0×10^5 cm	RADIUS
acceleration due to gravity	981.0 cm $\cdot$ s^{-2}	GRAV
angular velocity of the Earth's rotation	$\pi/43082.0$ radian $\cdot$ s^{-1}	OMEGA
the absolute temperature of 0 °C	273.15 K	TAB
the average density of sea water	1.036 g $\cdot$ cm^{-3}	RO
the specific heat of sea water	3.99×10^7 erg $\cdot$ g^{-1} $\cdot$ K^{-1} (1.0 erg $\cdot$ g^{-1} $\cdot$ K^{-1} $= 1.0 \times 10^{-4}$ J $\cdot$ kg^{-1} $\cdot$ K^{-1})	CP

Chapter 3

Spatial grid arrangement

MRI.COM uses a structured grid, and the model ocean domain is defined as a three-dimensional aggregate of rectangular grid cells on model's logical coordinate system. (However, for cells just above the bottom, so-called partial cells are used, which can locally change their vertical thickness.) The horizontal and vertical lengths of the cells are regarded as the horizontal and vertical grid intervals, respectively. In MRI.COM, the grid interval can be varied spatially in each direction (variable grid interval). Note that the introduction of z^* coordinate results in the temporally variable actual vertical grid intervals, though the logical grids are fixed in time.

In this chapter, we first describe the horizontal grid arrangement (3.1) and the vertical grid arrangement (3.2), which are main features of MRI.COM. Next, the notation of the grid index and the model region are shown (3.3). How to calculate the horizontal area of each grid (3.4) and the thickness and volume in the z^* coordinate system (3.5) are also explained. Finally, we summarize how to set the model grids for users (3.6).

3.1   Horizontal grid arrangement

MRI.COM adopts somewhat unique horizontal grid arrangement, which is illustrated in Figure 3.1a. Horizontal components of velocity and bottom depth are defined at the center of the grid cell ($\times$), and tracers such as temperature and salinity, density, and sea-surface height (SSH) are defined at the four corners of the cell ($\circ$). Hereafter, for simplicity, the velocity point is referred to as the U-point; the grid cell centered on the U-point, the U-cell (Figure 3.1c); the tracer point as the T-point; and the grid cell centered on the T-point, the T-cell (Figure 3.1c). The T-cells are staggered from the U-cells by a half grid size and consists of partial cells along the coast lines (Figure 3.2). The coast lines are defined by the periphery of the U-cells, i.e., the lines connecting the T-points. This type of horizontal grid arrangement is called Arakawa's B-grid arrangement (Arakawa, 1972). Although Arakawa's B-grid arrangement is also used in MOM (NOAA-GFDL, USA) and COCO (AORI of U. Tokyo and JAMSTEC, Japan), the primary cell is the T-cell in those models and the coast lines are defined by the lines connecting the U-points (Figure 3.1b).

In the case of the variable grid size, the T-points are defined just at the centers of the T-cells as seen in Figure 3.1c, but the U-points are not at the centers of the U-cells. The U-points are arranged so that the U-cell boundary stands at the mid-point between two neighboring U-points.

See Section 3.6.2 for the placement and numbering of the grid at the edge of the model domain.

3.2   Vertical grid arrangement

A variable grid size is usually used for the vertical grid arrangement, i.e., fine near the surface and coarse at depth. As illustrated in Figure 3.3a, tracers ($\circ$) and velocity ($\times$) are defined at just the mid-depth level of the cell, and the vertical mass fluxes W ($\triangle$, $\square$) are defined at the boundary of the cell. There are two kinds of W, one for the T-cell (W^T; $\triangle$) and another for the U-cell (W^U; $\square$). Their horizontal locations are the T-points and the U-points depicted in Figure 3.1a.

In order to express the gentle bottom slope as smoothly as possible, the thickness of the deepest U-cell at each horizontal location is variable (so called partial cell), with a limitation that it must exceed a fraction of around 10 percent of the nominal thickness of the layer to avoid violating the vertical CFL condition (Figure 3.3b). Otherwise, as presented in Figure 3.3c, the gentle bottom slope is expressed by wide, flat bottoms and cliffs here and there with height of vertical grid size Δz. In these regions, the vertical velocity is concentrated at the cliffs, resulting in relatively strong fictitious horizontal currents there.
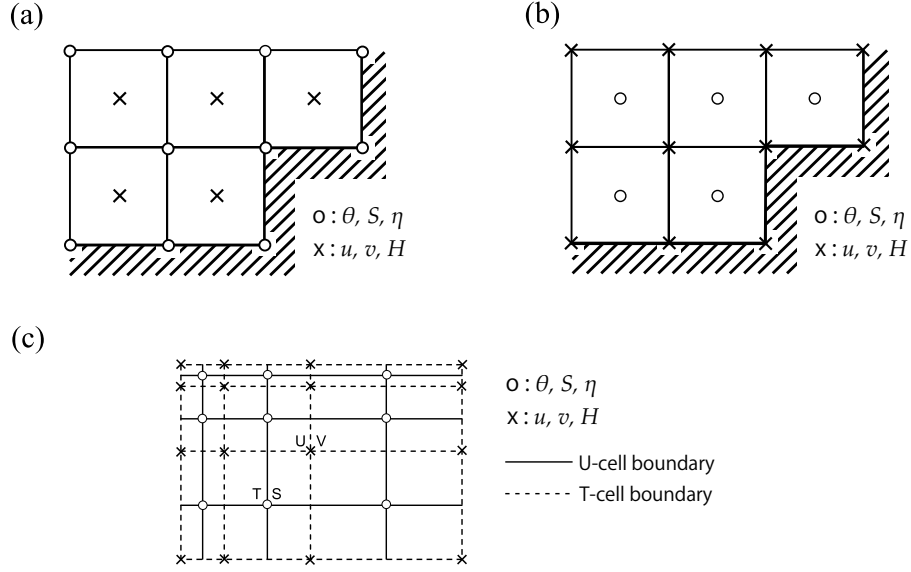
(a)

(b)

(c)

Figure3.1   Horizontal grid arrangement. (a) MRI.COM ($\circ : \theta, S, \eta$, $\times : u, v, H$), (b) MOM and COCO ($\circ : \theta, S, \eta, H$, $\times : u, v$), (c) Variable grid size in MRI.COM
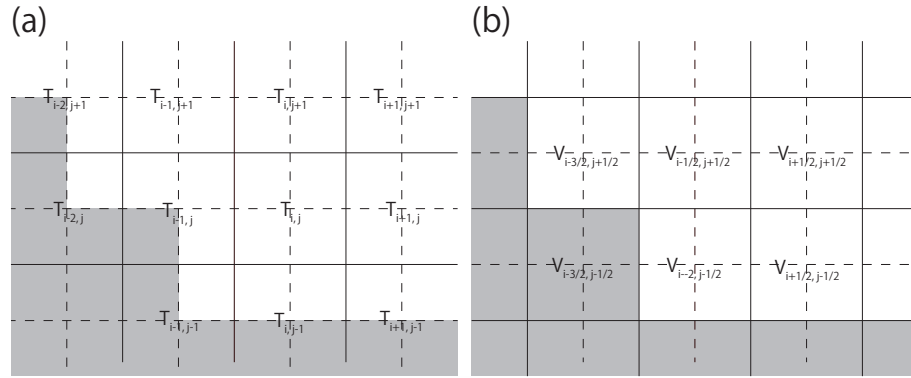
(a)

(b)

Figure3.2   Horizontal grid lattices in relation to topography. (a) Tracer lattice. (b) Velocity lattice. Land distribution (shade) is common for (a) and (b).

3.3   Grid indices and model domain

The conventions for indexing and the definitions of symbols used in finite difference expressions of the equations throughout this document are given here.

The actual distance corresponding to an increment of $\Delta\mu$ in the zonal direction of generalized orthogonal coordinates is expressed as follows:

$$\Delta x \equiv h_\mu \Delta \mu, \tag{3.1}$$

where h_μ is the scaling factor, the unit of which is [cm]. The unit of Δx is [cm], and $\Delta\mu$ is dimensionless. The actual meridional distance is defined similarly:

$$\Delta y \equiv h_\psi \Delta \psi. \tag{3.2}$$

The vertical distance is expressed by Δz (The unit is [cm]). For a discretized grid cell, the horizontal area is expressed by ΔA (= $\Delta x \Delta y$) and the volume is expressed by ΔV (= $\Delta x \Delta y \Delta z$).

The subscript indices expressing the horizontal grid position in the finite difference expression of the equations are usually integers for the T-points, i.e., (i, j) and are increased by a half for the U-points $(i + \frac{1}{2}, j + \frac{1}{2})$ (Figure 3.2). In some cases vice versa, with a notice.

In the vertical subscript index for the finite difference expression, the upper level of a grid cell, where the vertical mass flux is defined, is numbered as k ($k = 0$ being the sea surface), the levels of the T-point and U-point are numbered as $k - \frac{1}{2}$
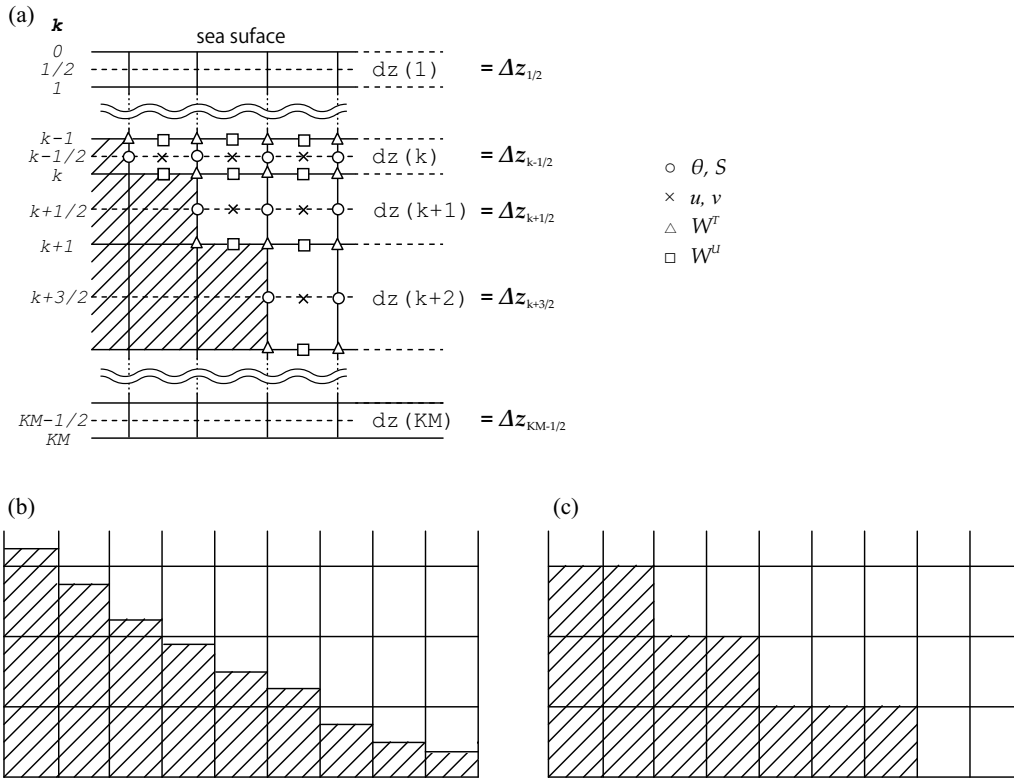
Figure3.3   Vertical grid arrangement. (a) Placement and numbering of vertical grid. (b) Smooth bottom slope with partial bottom cells. (c) Stair-like bottom slope.

(Figure 3.3a). In some cases, the T-point and U-point levels may be numbered as k, with a notice.

The model region is composed of U cells, and the numbers of horizontal grids (`imut`, `jmut`) are specified by the user (see Sec. 3.6). Note that this region includes the "halo region", which is the marginal region for the model calculation, in addition to the substantial "core region". The grid width of the halo region and the horizontal boundaries of the core region depend on the model settings as shown in Table 3.1. Figure 3.4a shows the model region of a closed basin surrounded by land, and Figure 3.4b shows that of a tri-polar global model. See Chapter 22 for more information on nested sub models.

Table3.1   Halo region and core region boundaries depending on model region settings.

model config	halo	west	east	south	north
closed basin (default)	1 grid-width land cell	$i = 2$	$i = \text{imut}$	$j = 2$	$j = \text{jmut}$
x-cyclic boundary condition (CYCLIC)	2 grids at east and west	$i = 3$	$i = \text{imut} - 1$	$j = 2$	$j = \text{jmut}$
tri-polar model (TRIPOLAR or JOT with CYCLIC)	2 grids at east and west, 1 at south, 3 at north	$i = 3$	$i = \text{imut} - 1$	$j = 2$	$j = \text{jmut} - 2$
nested sub model (SUB or OFFNESTSUB	2 grids at all boundaries	$i = 3$	$i = \text{imut} - 1$	$j = 3$	$j = \text{jmut} - 1$

3.4   Calculation of horizontal grid cell area and width

When equations are solved in MRI.COM, the temporal variations of physical quantities are calculated as a budget of their fluxes through the boundaries of the U-cells or T-cells (finite volume method). For this method, it is necessary to know the area and volume of the grid cells. These are numerically calculated for generalized orthogonal coordinate grids (Sec. 3.4.1), though they are analytically calculated if polar coordinate is chosen by user (Sec. 3.4.2). The outline of the lengths and areas calculated in this section is shown in the figure 3.5. Note that variable names in the program may be used even in the manual.
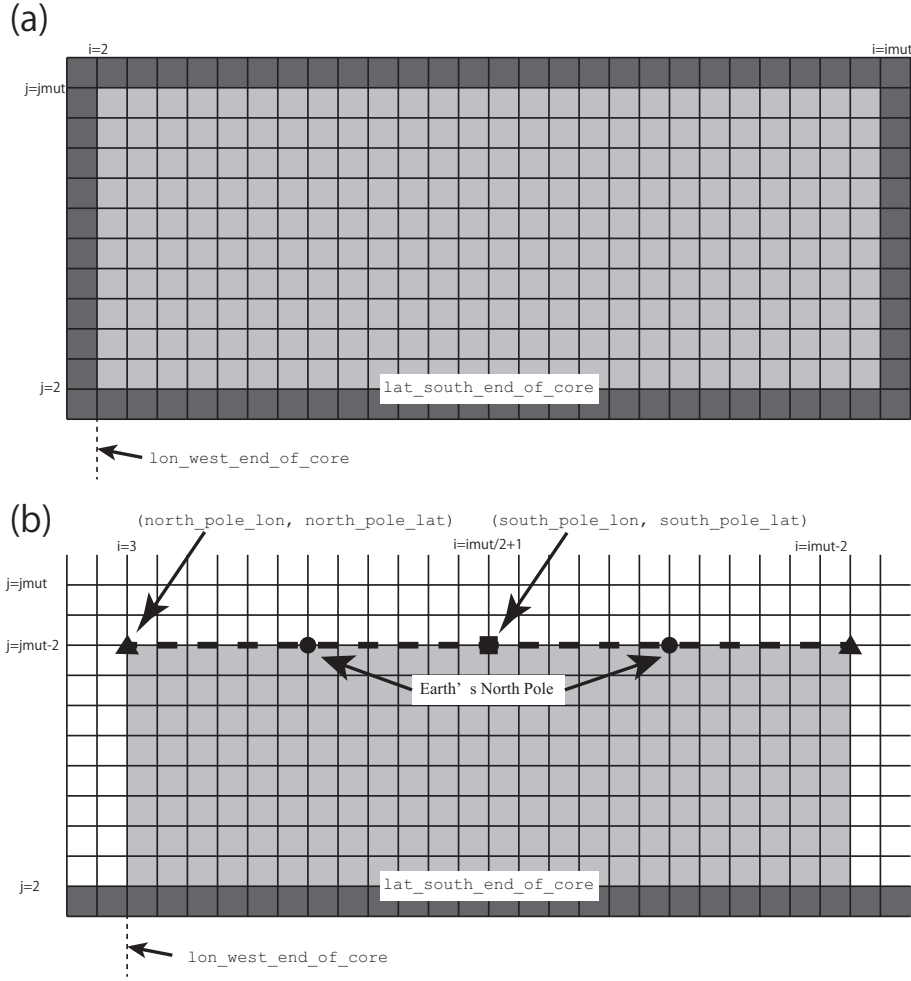
(a)

(b)

Figure3.4　The model domain and its halo region for (a) a model with closed domain, and (b) a tri-polar model with zonally cyclic (CYCLIC) and northern end folding (TRIPOLAR or JOT) conditions. The light shades are model's region of interest (core region). The dark shades are land that must be attached around the core region. The white cells in (b) are halo region. See Sec. 3.6 for the user specifications in the figure, such as north_pole_lon.

3.4.1　Generalized orthogonal coordinates

The longitude and latitude (λ, ϕ) of grid points on the sphere are defined by user as a function of the model coordinates (μ, ψ),

$$\lambda = \lambda(\mu, \psi), \quad \phi = \phi(\mu, \psi).$$

For example, the distance from a T-point $(\mu(i), \psi(j))$ to a point a half grid size to the east $(\mu(i + \frac{1}{2}), \psi(j))$ (variable name in the model: dx_bl; Figure 3.5a) is approximated numerically as follows taking $\mu_1 = \mu(i), \mu_2 = \mu(i + \frac{1}{2})$, and $\psi_1 = \psi(j)$:

$$\sum_{m=1}^{M} L\left[\lambda\left(\mu_1 + (m-1)\delta\mu, \psi_1\right), \phi\left(\mu_1 + (m-1)\delta\mu, \psi_1\right), \lambda\left(\mu_1 + m\delta\mu, \psi_1\right), \phi\left(\mu_1 + m\delta\mu, \psi_1\right)\right]. \tag{3.3}$$

Here, $L[\lambda_1, \phi_1, \lambda_2, \phi_2]$ is the distance between the two points (λ_1, ϕ_1) and (λ_2, ϕ_2) on the sphere along a great circle and $\delta\mu = (\mu_2 - \mu_1)/M$ (divided by $M \sim 20$ between μ_1 and μ_2).

Similarly, a quarter grid area (a_bl; Figure 3.5b) surrounded by four points $(\mu(i), \psi(j))$, $(\mu(i + \frac{1}{2}), \psi(j))$, $(\mu(i + \frac{1}{2}), \psi(j + \frac{1}{2}))$, and $(\mu(i), \psi(j + \frac{1}{2}))$ is, taking $\psi_2 = \psi(j + \frac{1}{2})$ and $\delta\psi = (\psi_2 - \psi_1)/N$ (divided by $N \sim 20$ between ψ_1 and
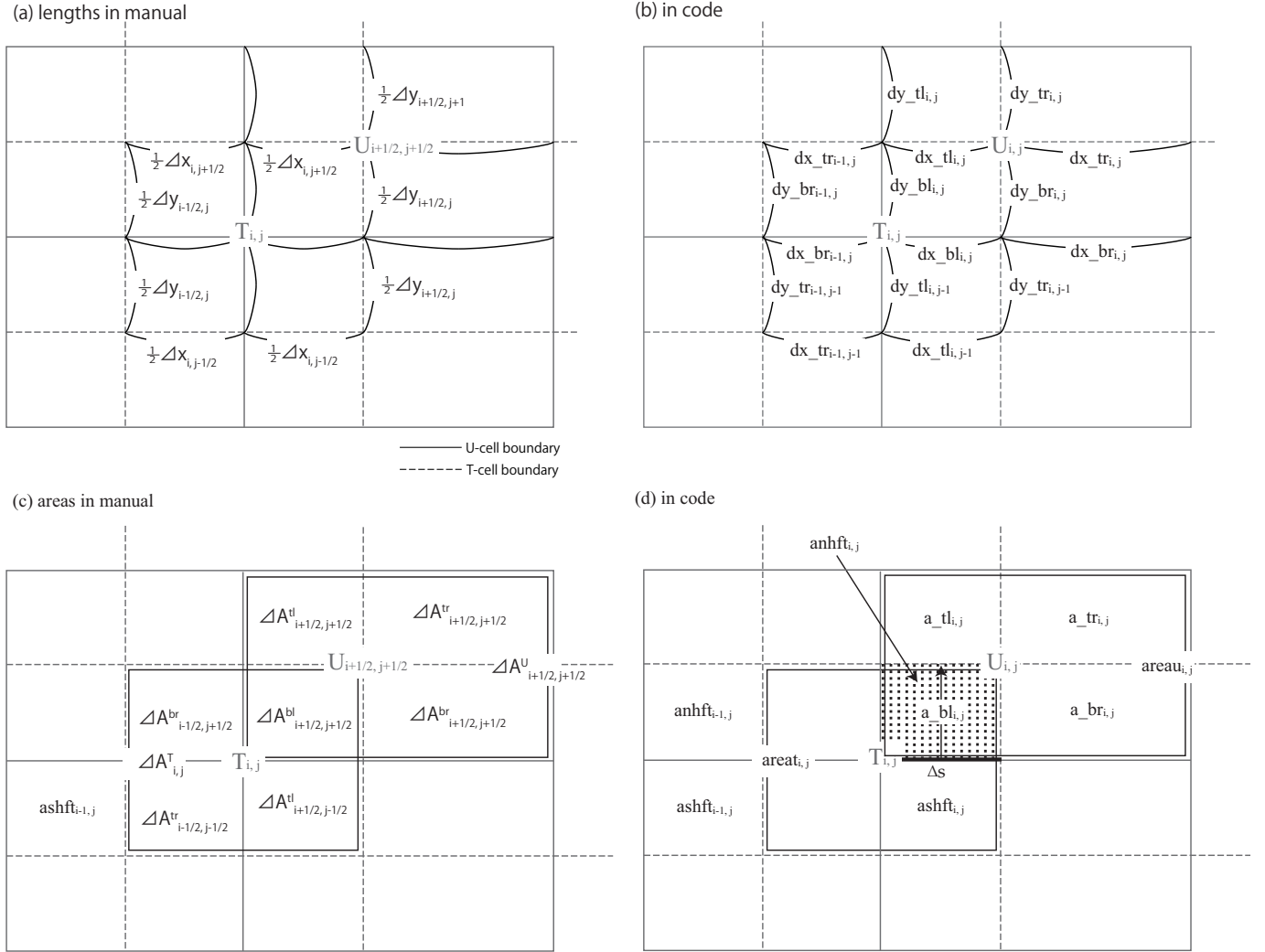
(a) lengths in manual

(b) in code

(c) areas in manual

(d) in code

Figure3.5   Variables that define a grid unit for (a)(b) distance $(\Delta x, \Delta y)$ and (c)(d) area (ΔA). The panels (a) and (c) show symbols and grid indices (i, j) following the convention described in Section 3.3. The panels (b) and (d) show variable names and indices in the code.

ψ_2), calculated as:

$$\sum_{n=1}^{N} \sum_{m=1}^{M} L\Big[\lambda\Big(\mu_1 + (m-1)\delta\mu, \psi_1 + \big(n - \tfrac{1}{2}\big)\delta\psi\Big), \qquad \phi\Big(\mu_1 + (m-1)\delta\mu, \psi_1 + \big(n - \tfrac{1}{2}\big)\delta\psi\Big),$$

$$\lambda\Big(\mu_1 + m\delta\mu, \psi_1 + \big(n - \tfrac{1}{2}\big)\delta\psi\Big), \qquad \phi\Big(\mu_1 + m\delta\mu, \psi_1 + \big(n - \tfrac{1}{2}\big)\delta\psi\Big)\Big]$$

$$\times$$

$$L\Big[\lambda\Big(\mu_1 + \big(m - \tfrac{1}{2}\big)\delta\mu, \psi_1 + (n-1)\delta\psi\Big), \qquad \phi\Big(\mu_1 + \big(m - \tfrac{1}{2}\big)\delta\mu, \psi_1 + (n-1)\delta\psi\Big),$$

$$\lambda\Big(\mu_1 + \big(m - \tfrac{1}{2}\big)\delta\mu, \psi_1 + n\delta\psi\Big), \qquad \phi\Big(\mu_1 + \big(m - \tfrac{1}{2}\big)\delta\mu, \psi_1 + n\delta\psi\Big)\Big]. \qquad (3.4)$$

As depicted in Figure 3.5, $(\mathtt{a\_bl})_{i,j}$ is the area of the lower left quarter of the central U-point. Those for the lower right $(\mathtt{a\_br})_{i,j}$, upper left $(\mathtt{a\_tl})_{i,j}$, and upper right $(\mathtt{a\_tr})_{i,j}$ quarters are obtained similarly.

The unit area centered on U-point $((\mathtt{areau})_{i,j})$ is then expressed as:

$$(\mathtt{areau})_{i,j} = (\mathtt{a\_bl})_{i,j} + (\mathtt{a\_br})_{i,j} + (\mathtt{a\_tl})_{i,j} + (\mathtt{a\_tr})_{i,j}, \qquad (3.5)$$

and the area centered on T-point $((\texttt{areat})_{i,j})$ as

$$(\texttt{areat})_{i,j} = (\texttt{a\_bl})_{i,j} + (\texttt{a\_br})_{i-1,j} + (\texttt{a\_tl})_{i,j-1} + (\texttt{a\_tr})_{i-1,j-1}. \tag{3.6}$$

Following the conventions for indexing introduced in Section 3.3 (i and j are notated with a half-grid shift for U points), the above equations are expressed in later chapters as follows:

$$\Delta A^U_{i+\frac{1}{2},j+\frac{1}{2}} = \Delta A^{bl}_{i+\frac{1}{2},j+\frac{1}{2}} + \Delta A^{br}_{i+\frac{1}{2},j+\frac{1}{2}} + \Delta A^{tl}_{i+\frac{1}{2},j+\frac{1}{2}} + \Delta A^{tr}_{i+\frac{1}{2},j+\frac{1}{2}}, \tag{3.7}$$

$$\Delta A^T_{i,j} = \Delta A^{bl}_{i+\frac{1}{2},j+\frac{1}{2}} + \Delta A^{br}_{i-\frac{1}{2},j+\frac{1}{2}} + \Delta A^{tl}_{i+\frac{1}{2},j-\frac{1}{2}} + \Delta A^{tr}_{i-\frac{1}{2},j-\frac{1}{2}}. \tag{3.8}$$

See Fig. 3.5.

3.4.2 Spherical coordinates

For grids in the spherical (geographic) coordinate system, we use more precise and computationally lighter analytical solutions. Let us examine the situation of T-cell divided in quarters (Figure 3.5). The area of the northeastern quarter (`anhft`, the same as that of the northwestern quarter) is obtained by the latitudinal integration of the thick line in Figure 3.5b, where $\Delta\phi = \phi(j + \frac{1}{2}) - \phi(j - \frac{1}{2})$.

Using the latitude of T-point $\phi(j)$, the zonal width of the grid unit for T-points $\Delta\lambda = \lambda(i + \frac{1}{2}) - \lambda(i - \frac{1}{2})$, and the Earth's radius a, the length of the thick line along the latitude circle (Δs) is expressed as:

$$\Delta s = a \frac{\Delta\lambda}{2} \cos\phi. \tag{3.9}$$

Integrating this in the latitudinal direction, we obtain the following.

$$
\begin{aligned}
(\texttt{anhft})_{i,j} &= \int_{\phi}^{\phi+\frac{\Delta\phi}{2}} \Delta s a\, d\phi = \frac{a^2 \Delta\lambda}{2} \int_{\phi}^{\phi+\frac{\Delta\phi}{2}} \cos\phi\, d\phi = \frac{a^2 \Delta\lambda}{2} \left\{ \sin\left(\phi + \frac{\Delta\phi}{2}\right) - \sin\phi \right\} \\
&= a^2 \Delta\lambda \cos\left(\phi + \frac{\Delta\phi}{4}\right) \sin\frac{\Delta\phi}{4} \\
&= a^2 \Delta\lambda \left(\cos\phi\cos\frac{\Delta\phi}{4} - \sin\phi\sin\frac{\Delta\phi}{4}\right) \sin\frac{\Delta\phi}{4} \\
&= a^2 \Delta\lambda \cos\phi\cos\frac{\Delta\phi}{4} \sin\frac{\Delta\phi}{4} \left(1 - \tan\phi\tan\frac{\Delta\phi}{4}\right) \\
&= \frac{a^2}{2} \Delta\lambda \cos\phi \sin\frac{\Delta\phi}{2} \left(1 - \tan\phi\tan\frac{\Delta\phi}{4}\right).
\end{aligned} \tag{3.10}
$$

Similarly, the area of the southeastern quarter of the T-cell (variable name in the model: `ashft`, the same as that of the southwestern quarter) is expressed as:

$$(\texttt{ashft})_{i,j} = \frac{a^2}{2} \Delta\lambda \cos\phi \sin\frac{\Delta\phi}{2} \left(1 + \tan\phi\tan\frac{\Delta\phi}{4}\right). \tag{3.11}$$

At the north and south poles, where $\phi = \pm 90°$, we obtain the following by changing (3.10) and (3.11) to the following forms.

$$(\texttt{anhft})_{i,j} = \frac{a^2}{2} \Delta\lambda \sin\frac{\Delta\phi}{2} \left(\cos\phi - \sin\phi\tan\frac{\Delta\phi}{4}\right) \tag{3.12}$$

$$(\texttt{ashft})_{i,j} = \frac{a^2}{2} \Delta\lambda \sin\frac{\Delta\phi}{2} \left(\cos\phi + \sin\phi\tan\frac{\Delta\phi}{4}\right). \tag{3.13}$$

At the north pole:

$$(\texttt{anhft})_{i,j} = 0 \tag{3.14}$$

$$(\texttt{ashft})_{i,j} = \frac{a^2}{2} \Delta\lambda \sin\frac{\Delta\phi}{2} \tan\frac{\Delta\phi}{4}. \tag{3.15}$$

At the south pole:

$$(\texttt{anhft})_{i,j} = \frac{a^2}{2} \Delta\lambda \sin\frac{\Delta\phi}{2}\tan\frac{\Delta\phi}{4} \tag{3.16}$$

$$(\texttt{ashft})_{i,j} = 0. \tag{3.17}$$

In our model

$$(\texttt{a\_bl})_{i,j} = (\texttt{anhft})_{i,j}, \qquad (\texttt{a\_br})_{i,j} = (\texttt{anhft})_{i+1,j},$$
$$(\texttt{a\_tl})_{i,j} = (\texttt{ashft})_{i,j+1}, \quad (\texttt{a\_tr})_{i,j} = (\texttt{ashft})_{i+1,j+1},$$

and the areas of the grid cells centered on the U-points and T-points are calculated by (3.5) and (3.6).

3.5   Calculation of vertical cell thickness

In the z^* coordinate system, the depth coordinate z from the seafloor $-H$ to the sea level η is converted to the z^* coordinate from $-H$ to 0 according to (Eq. 2.40). As a result, in the z^* coordinate system, the physical thickness Δz [cm] and the physical volume ΔV of each grid change depending on $\eta(t)$. In the following, how to calculate them are shown in the order of quarter grid unit, U cell, and T cell. Finally, the depth anomaly induced by ascending and descending of $\eta(t)$ is also shown. In the volume calculation, the area ΔA calculated by the method described in the previous section is used.

a. Distribute sea level variation to the four sub-divided parts of a T-cell

When the sea level variation $\eta_{i,j}$ is known at a T-point, the thicknesses of four divided cells that comprise a T-cell (i.e. four cells, $\Delta A^{bl}_{i+\frac{1}{2},j+\frac{1}{2}}, \Delta A^{tl}_{i+\frac{1}{2},j-\frac{1}{2}}, \Delta A^{br}_{i-\frac{1}{2},j+\frac{1}{2}}$ and $\Delta A^{tr}_{i-\frac{1}{2},j-\frac{1}{2}}$, in Fig. 3.5) are determined as follows:

$$(\texttt{dzu\_bl})_{i+\frac{1}{2},j+\frac{1}{2},k-\frac{1}{2}} = (\eta_{i,j} + H_{i+\frac{1}{2},j+\frac{1}{2}})\frac{(\texttt{dzu\_cnst})_{i+\frac{1}{2},j+\frac{1}{2},k-\frac{1}{2}}}{H_{i+\frac{1}{2},j+\frac{1}{2}}} \tag{3.18}$$

$$(\texttt{dzu\_tl})_{i+\frac{1}{2},j-\frac{1}{2},k-\frac{1}{2}} = (\eta_{i,j} + H_{i+\frac{1}{2},j-\frac{1}{2}})\frac{(\texttt{dzu\_cnst})_{i+\frac{1}{2},j-\frac{1}{2},k-\frac{1}{2}}}{H_{i+\frac{1}{2},j-\frac{1}{2}}} \tag{3.19}$$

$$(\texttt{dzu\_br})_{i-\frac{1}{2},j+\frac{1}{2},k-\frac{1}{2}} = (\eta_{i,j} + H_{i-\frac{1}{2},j+\frac{1}{2}})\frac{(\texttt{dzu\_cnst})_{i-\frac{1}{2},j+\frac{1}{2},k-\frac{1}{2}}}{H_{i-\frac{1}{2},j+\frac{1}{2}}} \tag{3.20}$$

$$(\texttt{dzu\_tr})_{i-\frac{1}{2},j-\frac{1}{2},k-\frac{1}{2}} = (\eta_{i,j} + H_{i-\frac{1}{2},j-\frac{1}{2}})\frac{(\texttt{dzu\_cnst})_{i-\frac{1}{2},j-\frac{1}{2},k-\frac{1}{2}}}{H_{i-\frac{1}{2},j-\frac{1}{2}}}, \tag{3.21}$$

where H is the depth of sea floor and $\texttt{dzu\_cnst}$ at U-points is the logical definition of vertical cell thickness in z^* frame, which does not vary in time. Volume of the four cells becomes

$$(\texttt{volu\_bl})_{i+\frac{1}{2},j+\frac{1}{2},k-\frac{1}{2}} = \Delta A^{bl}_{i+\frac{1}{2},j+\frac{1}{2}}(\texttt{dzu\_bl})_{i+\frac{1}{2},j+\frac{1}{2},k-\frac{1}{2}} \tag{3.22}$$

$$(\texttt{volu\_tl})_{i+\frac{1}{2},j-\frac{1}{2},k-\frac{1}{2}} = \Delta A^{tl}_{i+\frac{1}{2},j-\frac{1}{2}}(\texttt{dzu\_tl})_{i+\frac{1}{2},j-\frac{1}{2},k-\frac{1}{2}} \tag{3.23}$$

$$(\texttt{volu\_br})_{i-\frac{1}{2},j+\frac{1}{2},k-\frac{1}{2}} = \Delta A^{br}_{i-\frac{1}{2},j+\frac{1}{2}}(\texttt{dzu\_br})_{i-\frac{1}{2},j+\frac{1}{2},k-\frac{1}{2}} \tag{3.24}$$

$$(\texttt{volu\_tr})_{i-\frac{1}{2},j-\frac{1}{2},k-\frac{1}{2}} = \Delta A^{tr}_{i-\frac{1}{2},j-\frac{1}{2}}(\texttt{dzu\_tr})_{i-\frac{1}{2},j-\frac{1}{2},k-\frac{1}{2}}. \tag{3.25}$$

Using these, the new volume of T-cells and U-cells is obtained. There is no leak in volume by using this method. Figure 3.6 illustrates the procedure.

b. U-cell

Thickness of a U-cell ($\texttt{dzu}$) is obtained by dividing U-cell's volume by U-cell's horizontal area. U-cell's volume is a sum of the four sub-divided cells whose volume varies following sea level variation on T-cells where they belong to. Using (3.22) through (3.25), we have,

$$(\texttt{volu})_{i+\frac{1}{2},j+\frac{1}{2},k-\frac{1}{2}} = (\texttt{volu\_bl})_{i+\frac{1}{2},j+\frac{1}{2},k-\frac{1}{2}} + (\texttt{volu\_br})_{i+\frac{1}{2},j+\frac{1}{2},k-\frac{1}{2}}$$
$$+ (\texttt{volu\_tl})_{i+\frac{1}{2},j+\frac{1}{2},k-\frac{1}{2}} + (\texttt{volu\_tr})_{i+\frac{1}{2},j+\frac{1}{2},k-\frac{1}{2}}. \tag{3.26}$$

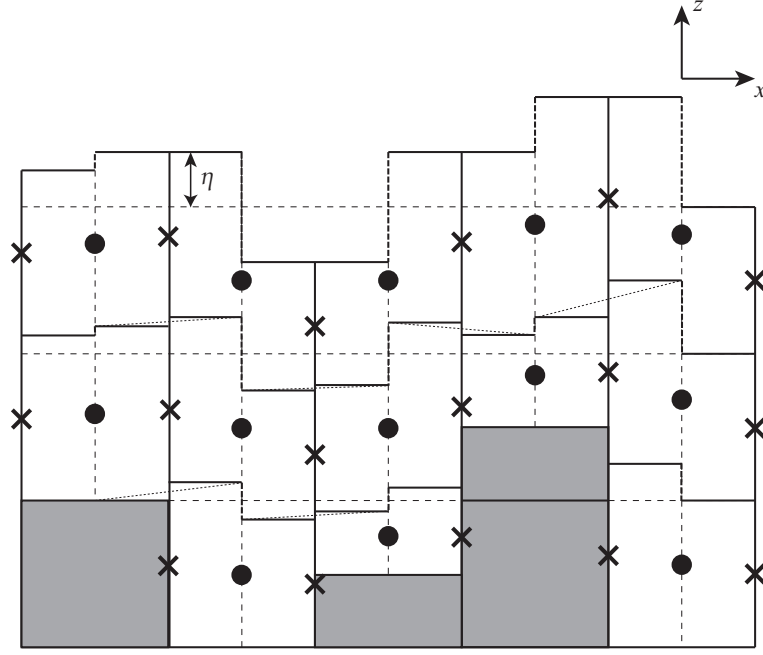Figure3.6   Illustration of a vertical slice through a set of grid cells in the x-z plane for z^* coordinate. The center point in each cell ($\bullet$) is a velocity point. The cross ($\times$) is a tracer point.

Then the thickness is computed by

$$(\texttt{dzu})_{i+\frac{1}{2},j+\frac{1}{2},k-\frac{1}{2}} \equiv (\texttt{volu})_{i+\frac{1}{2},j+\frac{1}{2},k-\frac{1}{2}} \Big/ (\texttt{areau})_{i+\frac{1}{2},j+\frac{1}{2}}, \tag{3.27}$$

that is, the thickness of a U-cell is the average of the thickness of the four sub-divided T-cells.

c. T-cell

Volume of a T-cell is also calculated as a sum of the four sub-divided cells. Using (3.22) through (3.25), we have

$$\begin{aligned}(\texttt{volt})_{i,j,k-\frac{1}{2}} = {}&(\texttt{volu\_bl})_{i+\frac{1}{2},j+\frac{1}{2},k-\frac{1}{2}} + (\texttt{volu\_tl})_{i+\frac{1}{2},j-\frac{1}{2},k-\frac{1}{2}} \\ &+ (\texttt{volu\_br})_{i-\frac{1}{2},j+\frac{1}{2},k-\frac{1}{2}} + (\texttt{volu\_tr})_{i-\frac{1}{2},j-\frac{1}{2},k-\frac{1}{2}}.\end{aligned} \tag{3.28}$$

Because horizontal cross section of a T-cell is not uniform vertically owing to the presence of partial cells, thickness of a T-cell cannot be determined identically. Here, the thickness $\texttt{dzt\_cnst}$ is determined as the difference between top and bottom face of the T-cell,

$$\begin{aligned}(\texttt{dzt\_cnst})_{i,j,k-\frac{1}{2}} = \max\big(&(\texttt{dzu\_cnst})_{i+\frac{1}{2},j+\frac{1}{2},k-\frac{1}{2}}, (\texttt{dzu\_cnst})_{i+\frac{1}{2},j-\frac{1}{2},k-\frac{1}{2}}, \\ &(\texttt{dzu\_cnst})_{i-\frac{1}{2},j+\frac{1}{2},k-\frac{1}{2}}, (\texttt{dzu\_cnst})_{i-\frac{1}{2},j-\frac{1}{2},k-\frac{1}{2}}\big).\end{aligned} \tag{3.29}$$

d. Depth anomalies

We defined vertical cell thickness of four divided cells that comprise a T-cell by (3.18) through (3.21). In the same manner, we may define the anomalies of the actual depth at the center and bottom of the four divided cells, with $-\eta$ at the sea surface ($s = 0$). Note that depth is defined positive downward.

For the center,

$$(\texttt{dpu\_bl})_{i+\frac{1}{2},j+\frac{1}{2},k-\frac{1}{2}} = -\frac{H_{i+\frac{1}{2},j+\frac{1}{2}} - (\texttt{dpu\_cnst})_{i+\frac{1}{2},j+\frac{1}{2},k-\frac{1}{2}}}{H_{i+\frac{1}{2},j+\frac{1}{2}}}\eta_{i,j} \tag{3.30}$$

$$(\texttt{dpu\_tl})_{i+\frac{1}{2},j-\frac{1}{2},k-\frac{1}{2}} = -\frac{H_{i+\frac{1}{2},j-\frac{1}{2}} - (\texttt{dpu\_cnst})_{i+\frac{1}{2},j-\frac{1}{2},k-\frac{1}{2}}}{H_{i+\frac{1}{2},j-\frac{1}{2}}}\eta_{i,j} \tag{3.31}$$

$$(\texttt{dpu\_br})_{i-\frac{1}{2},j+\frac{1}{2},k-\frac{1}{2}} = -\frac{H_{i-\frac{1}{2},j+\frac{1}{2}} - (\texttt{dpu\_cnst})_{i-\frac{1}{2},j+\frac{1}{2},k-\frac{1}{2}}}{H_{i-\frac{1}{2},j+\frac{1}{2}}}\eta_{i,j} \tag{3.32}$$

$$(\texttt{dpu\_tr})_{i-\frac{1}{2},j-\frac{1}{2},k-\frac{1}{2}} = -\frac{H_{i-\frac{1}{2},j-\frac{1}{2}} - (\texttt{dpu\_cnst})_{i-\frac{1}{2},j-\frac{1}{2},k-\frac{1}{2}}}{H_{i-\frac{1}{2},j-\frac{1}{2}}}\eta_{i,j} \tag{3.33}$$

and for the bottom,

$$(\texttt{depu\_bl})_{i+\frac{1}{2},j+\frac{1}{2},k} = -\frac{H_{i+\frac{1}{2},j+\frac{1}{2}} - (\texttt{depu\_cnst})_{i+\frac{1}{2},j+\frac{1}{2},k}}{H_{i+\frac{1}{2},j+\frac{1}{2}}}\eta_{i,j} \tag{3.34}$$

$$(\texttt{depu\_tl})_{i+\frac{1}{2},j-\frac{1}{2},k} = -\frac{H_{i+\frac{1}{2},j-\frac{1}{2}} - (\texttt{depu\_cnst})_{i+\frac{1}{2},j-\frac{1}{2},k}}{H_{i+\frac{1}{2},j-\frac{1}{2}}}\eta_{i,j} \tag{3.35}$$

$$(\texttt{depu\_br})_{i-\frac{1}{2},j+\frac{1}{2},k} = -\frac{H_{i-\frac{1}{2},j+\frac{1}{2}} - (\texttt{depu\_cnst})_{i-\frac{1}{2},j+\frac{1}{2},k}}{H_{i-\frac{1}{2},j+\frac{1}{2}}}\eta_{i,j} \tag{3.36}$$

$$(\texttt{depu\_tr})_{i-\frac{1}{2},j-\frac{1}{2},k} = -\frac{H_{i-\frac{1}{2},j-\frac{1}{2}} - (\texttt{depu\_cnst})_{i-\frac{1}{2},j-\frac{1}{2},k}}{H_{i-\frac{1}{2},j-\frac{1}{2}}}\eta_{i,j}, \tag{3.37}$$

where $\texttt{dpu\_cnst}$ is the logical depth at the center of a U-cell (dashed line in Figure 3.3a) and $\texttt{depu\_cnst}$ is the logical depth at the bottom of a U-cell (solid line in Figure 3.3a).

The depth anomaly of a T-point is obtained as an area average. For example, at the center,

$$(\texttt{dpt})_{i,j,k-\frac{1}{2}} = \Big\{(\texttt{a\_bl})_{i+\frac{1}{2},j+\frac{1}{2}}(\texttt{dpu\_bl})_{i+\frac{1}{2},j+\frac{1}{2},k-\frac{1}{2}} + (\texttt{a\_tl})_{i+\frac{1}{2},j-\frac{1}{2}}(\texttt{dpu\_tl})_{i+\frac{1}{2},j-\frac{1}{2},k-\frac{1}{2}}$$
$$+ (\texttt{a\_br})_{i-\frac{1}{2},j+\frac{1}{2}}(\texttt{dpu\_br})_{i-\frac{1}{2},j+\frac{1}{2},k-\frac{1}{2}} + (\texttt{a\_tr})_{i-\frac{1}{2},j-\frac{1}{2}}(\texttt{dpu\_tr})_{i-\frac{1}{2},j-\frac{1}{2},k-\frac{1}{2}}\Big\}/(\texttt{areat})_{i,j,k+\frac{1}{2}} \tag{3.38}$$

and for the bottom,

$$(\texttt{dept})_{i,j,k} = \Big\{(\texttt{a\_bl})_{i+\frac{1}{2},j+\frac{1}{2}}(\texttt{depu\_bl})_{i+\frac{1}{2},j+\frac{1}{2},k} + (\texttt{a\_tl})_{i+\frac{1}{2},j-\frac{1}{2}}(\texttt{depu\_tl})_{i+\frac{1}{2},j-\frac{1}{2},k}$$
$$+ (\texttt{a\_br})_{i-\frac{1}{2},j+\frac{1}{2}}(\texttt{depu\_br})_{i-\frac{1}{2},j+\frac{1}{2},k} + (\texttt{a\_tr})_{i-\frac{1}{2},j-\frac{1}{2}}(\texttt{depu\_tr})_{i-\frac{1}{2},j-\frac{1}{2},k}\Big\}/(\texttt{areat})_{i,j,k+\frac{1}{2}}. \tag{3.39}$$

In the above calculation, we use only full cells, that is, we do not include partial cells except for the bottom cell ($k = ktbtm$). This is reflected in the use of $(\texttt{areat})_{i,j,k+\frac{1}{2}}$ instead of $(\texttt{areat})_{i,j,k-\frac{1}{2}}$.

Using this, the variable thickness of a T-cell is calculated as follows:

$$(\texttt{dzt})_{i,j,k-\frac{1}{2}} = (\texttt{dept})_{i,j,k} - (\texttt{dept})_{i,j,k-1} + (\texttt{dzt\_cnst})_{i,j,k-\frac{1}{2}}. \tag{3.40}$$

3.6   Usage

How to set the model region and grid are explained here. Specifically, the horizontal coordinate system is selected in Sec. (3.6.1), and the region and grid are set in Sec. (3.6.2). Also, if a polar coordinate is not used, the user must provide the grid width and area directly in Sec. (3.6.3).

3.6.1   Horizontal coordinate system

For horizontal coordinate system, either spherical or generalized orthogonal curvilinear coordinates must be chosen.

a. Spherical coordinates

For a model that does not include the North Pole, spherical coordinates with geographical longitude-latitude axes will be a standard choice.

If spherical coordinates are chosen, model option `SPHERICAL` must be added to the list of options (the line start with `OPTIONS =`) specified in `configure.in`.

The geographical position of north and south pole should not be necessarily at the Earth's North and South Pole. If the model's north pole is displaced, this is specified by namelist `nml_poles` (Table 3.2).

Table3.2 Namelist `nml_poles` for `SPHERICAL` option. The geographical location of the model's south pole is determined automatically by the specification of the north pole.

variable name	units	description	usage
north_pole_lon	degree	geographical longitude of north pole	default is 0°
north_pole_lat	degree	geographical latitude of north pole	default is 90°N

b. Generalized orthogonal curvilinear coordinates

Singularity at the North Pole may be avoided by coordinate transformation within the framework of generalized orthogonal curvilinear coordinates.

Two options are available:

- Tripolar grid (`TRIPOLAR`) combining geographical lat-lon south of around 60°N and transformed coordinates to the north.
- Joukowski conversion (`JOT`) applied to the whole sphere of the Earth.

When either `TRIPOLAR` or `JOT` option is chosen, that option must be added to the list of options (the line start with `OPTIONS =`) specified in `configure.in`. In addition, namelist `nml_poles` must be specified, but in this case the geographical locations of the two new singular points instead of the Earth's North and South Pole should be given (Table 3.3). See Chapter 24 for details.

Table3.3 Namelist `nml_poles` for `TRIPOLAR` or `JOT` option. See also Figure 3.4b for the locations of the two singular points to be specified.

variable name	units	description	usage
north_pole_lon	degree	geographical longitude of one of the two new singular points	specification is required
north_pole_lat	degree	geographical latitude of one of the two new singular points	specification is required
south_pole_lon	degree	geographical longitude of the other of the two new singular points	specification is required
south_pole_lat	degree	geographical latitude of the other of the two new singular points	specification is required

3.6.2 Model domain and grid

There are several options about the model region as shown in Table 3.1: closed basin (default), *x*-cyclic boundary condition(`CYCLIC`), tri-pole models (`TRIPOLAR`) and nested sub models (`SUB` or `OFFNESTSUB`). User specifies these options in `configure.in`.

The total numbers of grid points in the three directions (`imut`, `jmut`, and `km`) must be given to `configure.in`, too. The grid sizes (`imut` and `jmut`) must include halo cells. Minimum information that must be given to `configure.in` for compiling a global tri-polar grid model will look like as follows.

```
─────────── An example specification given to configure.in for a global tri-polar grid model ───────────

 OPTIONS="TRIPOLAR CYCLIC"
 IMUT=364
 JMUT=368
 KM=60
```

Further horizontal grid information is given to the model by namelist at run time. It is necessary to specify the western and southern end of model's core region and the X and Y axis grid spacing. They are given by namelist `nml_horz_grid` (Table 3.4). When the horizontal grid spacing is given by a file, the file is read by the model at run time as follows.

```
─────────── Format of horizontal grid spacing data (file_dxdy_tbox_deg). ───────────

    real(8) :: dxtdeg(imut), dytdeg(jmut)
    integer(4),parameter :: lun = 10
    open(lun, file=file_dxdy_tbox_deg, form=unformatted )
    read( lun ) i, j
    if ( ( i == imut ).and.( j == jmut ) ) then
      read( lun ) dxtdeg
      read( lun ) dytdeg
    end if
    close(lun)
```

Here, `dxtdeg` and `dytdeg` are longitudinal and latitudinal width of T-cells, respectively (Figure 3.4c). Note that they can vary only in the direction of their own axis.

Table3.4   Namelist `nml_horz_grid`

variable name	units	description	usage
lon_west_end_of_core	model longitude in degree	the longitude of the western end of model's main region	specification is required
lat_south_end_of_core	model latitude in degree	the latitude of the southern end of model's main region	specification is required
dx_const_deg	degree	uniform X-axis grid spacing	default is zero
dy_const_deg	degree	uniform Y-axis grid spacing	default is zero
file_dxdy_tbox_deg	character	X and Y axis grid spacing are given by this file	If either X or Y axis grid spacing is not uniform, prepare this file.

The vertical water column is filled by U-cells with specified thickness. The start point of the vertical grid is always set to be zero (sea surface). The vertical grid index increases downward and the vertical grid width ($\Delta z_{k-\frac{1}{2}} = $ `dz(k)`) is given either by a file or a namelist. Which one to select is determined by namelist `nml_vert_grid` (Table 3.5) at run time. When the vertical grid spacing is given by a file, the file is read by the model at run time as follows.

```
─────────── Format of vertical grid spacing data (file_dz_cm). ───────────

    real(8) :: dz(km)
    integer(4),parameter :: lun = 10
    open(lun, file=file_dz_cm, form=unformatted)
    read(lun) k
    if ( k == km ) then
      read(lun) dz
    endif
    close(lun)
```

3.6.3   Grid cell area and line elements

When spherical coordinates are chosen (SPHERICAL), grid cell area and line elements are calculated analytically by the model (Section 3.4.2). When generalized orthogonal curvilinear coordinates are chosen (TRIPOLAR or JOT), they should be read from file (Section 3.4.1). The file name must be given by namelist `nml_grid_scale` (Table 3.6).
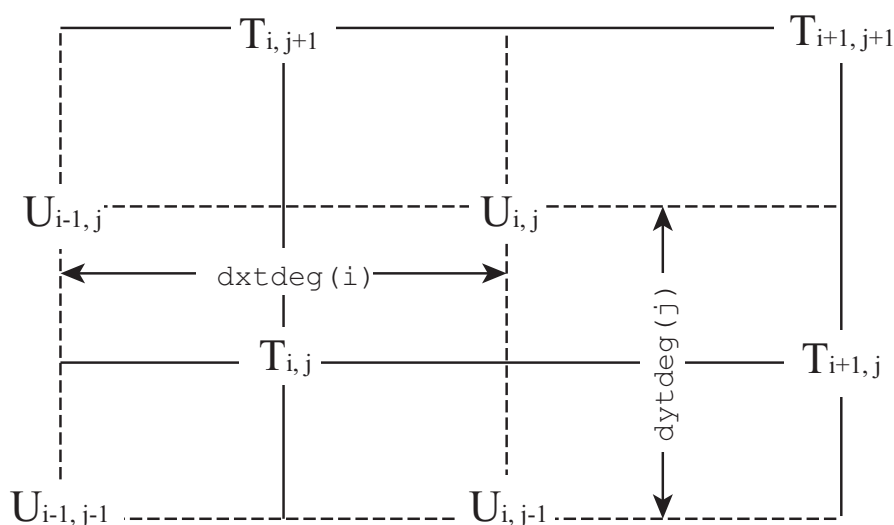
Figure3.7　Specification of the basic arrays (`dxtdeg` and `dytdeg`) that define grid spacing. Grid indices (i, j) follow array indices in program codes. The indices of the T-points in the vicinity of boundaries are shown in Fig. 3.4.

Table3.5　Namelist `nml_vert_grid`

variable name	units	description	usage
`file_dz_cm`	character	vertical grid spacing is given by this file	If the vertical grid spacing is not uniform, prepare this file. `dz_const_cm` must not be given.
`dz_const_cm`	cm	uniform vertical grid spacing	default is zero

Table3.6　Namelist `nml_grid_scale`

variable name	units	description	usage
`file_scale`	character	grid cell area and line elements are given by this file	specification is required for `TRIPOLAR` or `JOT`.

The file that contains the grid cell and line elements (see also Figure 3.5 for positions) is read by the model at run time as follows.

Chapter 3   Spatial grid arrangement

―――――― Format of grid cell area and line elements (`file_scale`; if not SPHERICAL) ――――――

```
real(8) :: a_bl(imut,jmut),  a_br(imut,jmut),  a_tl(imut,jmut),  a_tr(imut,jmut)
real(8) :: dx_bl(imut,jmut), dx_br(imut,jmut), dx_tl(imut,jmut), dx_tr(imut,jmut)
real(8) :: dy_bl(imut,jmut), dy_br(imut,jmut), dy_tl(imut,jmut), dy_tr(imut,jmut)
integer(4),parameter :: lun = 10
open(unit=lun, file=file_scale, form=unformatted)
read(unit=lun) a_bl  ! U-box area of bottom-left 1/4 grid
read(unit=lun) a_br  ! U-box area of bottom-right 1/4 grid
read(unit=lun) a_tl  ! U-box area of top-left 1/4 grid
read(unit=lun) a_tr  ! U-box area of top-right 1/4 grid
read(unit=lun) dx_bl ! U-box length of bottom-left 1/4 grid
read(unit=lun) dx_br ! U-box length of bottom-right 1/4 grid
read(unit=lun) dx_tl ! U-box length of top-left 1/4 grid
read(unit=lun) dx_tr ! U-box length of top-right 1/4 grid
read(unit=lun) dy_bl ! U-box length of bottom-left 1/4 grid
read(unit=lun) dy_br ! U-box length of bottom-right 1/4 grid
read(unit=lun) dy_tl ! U-box length of top-left 1/4 grid
read(unit=lun) dy_tr ! U-box length of top-right 1/4 grid
close(lun)
```

Chapter 4

Time integration

In this chapter, we discuss the time integration method for the primitive equations defined in Section 2.2. In Section 4.2, we discuss the leap-frog scheme, which is traditionally used in ocean models and has been used in MRI.COM until version 4.7. Section 4.3 describes the Leap frog Adams-Moulton (LFAM3) scheme, which was first used in ocean models by the Regional Ocean Modeling System (ROMS) and has become the only time integration scheme in MRI.COM since version 5.0.

4.1 Time integration flow

In MRI.COM, each component is calculated as follows.

1. Boundary Process (Part V) + Sea ice (Chapter 17)
2. **Evolution of tracers (Part IV)**
3. **Equation of state (Chapter 5)**
4. **Equation of motion [baroclinic component] (Chapter 8)**
5. **Equation of motion [barotropic component] (Chapter 7)**
6. Turbulence closure models (Chapter 15)
7. **Preparing for the next step**

However, the sea ice and mixed layer calculations are always done in forward differencing, independent of the time integration scheme of the ocean model. This is especially important for sea ice to satisfy conservation laws. For details, see section 17 for sea ice and section 15 for the mixed layer. Only for the remaining items, marked with **bold line**, the ocean model time integration scheme is applied.

4.2 Leap-frog method (LF)

For the time integration method of MRI.COM, the leap-frog method (LF) had been used until version 4.7.

Consider the following typical advection-diffusion equation (the first term on the right-hand side is advection and the second term on the right-hand side is diffusion)

$$\frac{\partial a}{\partial t} = \mathcal{A}(a) + \mathcal{D}(a) \tag{4.1}$$

Three time steps are used in solving this equation.

$$a^{n+1} = a^{n-1} + 2\Delta t \times \left\{ \mathcal{A}(a^n) + \mathcal{D}(a^{n-1}) \right\} \tag{4.2}$$

This method has long been the standard for ocean models because it is simple, energy-neutral, and one of the most computationally efficient method to describe wave equations. However, there are some problems. The accuracy is only $O(\Delta t^2)$. Since the time series of a^{2n+1} and a^{2n} are separated (red and blue lines in Fig. 4.1), it is difficult to satisfy the conservation between the two time series. Before this problem becomes serious, a Matsuno scheme consisting of two steps, forward scheme and backward scheme, is inserted once in the calculation of a few dozen steps in LF, so that one of the separated modes is discarded. The Matsuno scheme is also used to create the two time steps needed for LF at the start of integration. In addition, the accurate advection of tracers is often written in forward difference method, in which case the stability is halved. The issue of conservation is a particularly serious problem when fluxes are exchanged with other systems that are not running in LF, such as sea ice. In order to solve these problems, starting with 5.0, we will use the third order leap-frog Adams-Moulton (LFAM3), which is used in Regional Ocean Models (ROMS).
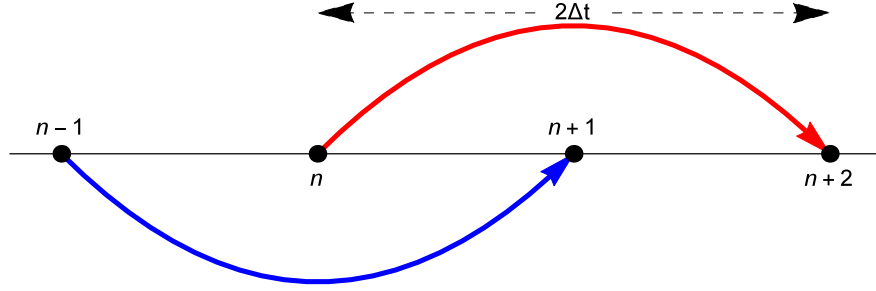
Figure4.1   Schematic description of the LF time integration.

4.3   Leap-frog Adams-Moulton (LFAM3) method

Consider the following one-dimensional wave equation,

$$\frac{\partial p}{\partial t} = -c\frac{\partial u}{\partial x}, \tag{4.3}$$

$$\frac{\partial u}{\partial t} = -c\frac{\partial p}{\partial x}. \tag{4.4}$$

where p is pressure, u is velocity, and c is the phase velocity of the wave. Applying the Fourier transformation with respect to space by placing $p(t,x) = \hat{p}_k e^{ikx}, u(t,x) = \hat{u}_k u^{ikx}$ and $\omega_k = kc$ yields,

$$\frac{\partial \hat{p}_k}{\partial t} = -i\omega_k \hat{u}_k, \tag{4.5}$$

$$\frac{\partial \hat{u}_k}{\partial t} = -i\omega_k \hat{p}_k. \tag{4.6}$$

For simplicity, we omit ˆ and the subscript k, and denote the variable ζ^n at the time $t = n\Delta t$ of the variable ζ. To further simplify the equation, we introduce the dimensionless quantity $\alpha = \omega_k \Delta t$.

The LFAM3 for the Fourier transform of the 1D wave equation with respect to space is written as follows. These equations correspond to equations (2.38)-(2.41) in Shchepetkin and McWilliams (2005) (hereafter, SM2005) (or equations (4.1)-(4.2) in Shchepetkin and McWilliams (2009) (hereafter, SM2009)). The derivation of these equations is included in Chapter 23 of this manual (23.49–23.52).

LFAM3 is composed of the predictor substep:

$$p^{n+\frac{1}{2}} = \left(\frac{1}{2} - 2\gamma\right)p^{n-1} + \left(\frac{1}{2} + 2\gamma\right)p^n - i\alpha(1 - 2\gamma)u^n \tag{4.7}$$

$$u^{n+\frac{1}{2}} = \left(\frac{1}{2} - 2\gamma\right)u^{n-1} + \left(\frac{1}{2} + 2\gamma\right)u^n - i\alpha(1 - 2\gamma)\left[p^n + \beta\frac{2p^{n+1/2} - 3p^n + p^{n-1}}{1 - 2\gamma}\right] \tag{4.8}$$

and the corrector substep:

$$p^{n+1} = p^n - i\alpha u^{n+\frac{1}{2}} \tag{4.9}$$

$$u^{n+1} = u^n - i\alpha\left\{(1 - \epsilon)p^{n+\frac{1}{2}} + \epsilon\left[\left(\frac{1}{2} - \gamma\right)p^{n+1} + \left(\frac{1}{2} + 2\gamma\right)p^n - \gamma p^{n-1}\right]\right\}, \tag{4.10}$$
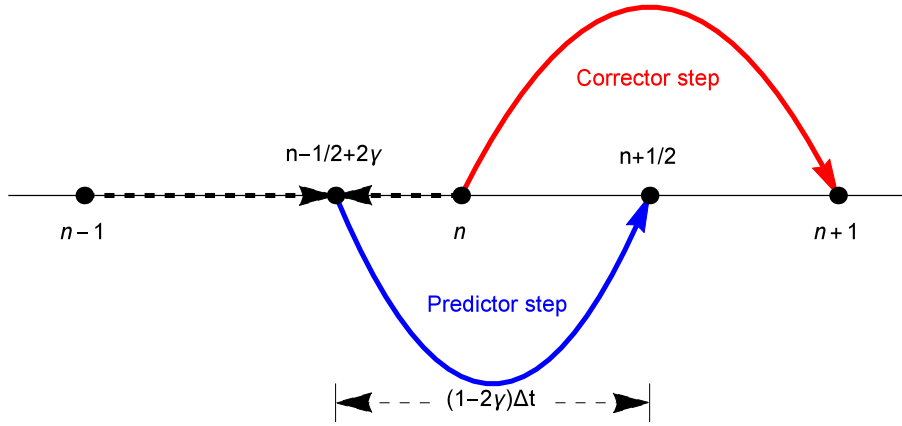
Figure4.2　Schematic description of the LFAM3 time integration. During the predictor substep, the initial data at $n-1$ and n steps are linearly interpolated to $n-\frac{1}{2}+2\gamma$ step and advanced to $n+\frac{1}{2}$ step by $(1-2\gamma)\Delta t$. During the corrector substep, the resultant values are used to compute the RHS at $n+\frac{1}{2}$ step to advance prognostic variables from n to $n+1$ steps. At the end of the corrector substep, the values at $n+\frac{1}{2}$ step are discarded.

where $\alpha = kc\Delta t$. The u corresponds to the flow velocity and p corresponds to the active tracer (temperature, salinity) related to the pressure. The predictor substep for $p^{n+\frac{1}{2}}$ can be interpreted as the time integration from $n-\frac{1}{2}+2\gamma$ step to $n = n-\frac{1}{2}$ step by $(1-2\gamma)\Delta t$ (Figure4.2).

During the corrector substep of finding p^{n+1}, the time integration for the advection is conducted from n to $n+1$step using velocity at $n+\frac{1}{2}$ step, which is compatible with high accurate tracer advection schemes such as Second Order Moments (SOM). During the corrector step of finding u^{n+1}, the values for the pressure gradient term is a linear combination of $n-1$, n, $n+\frac{1}{2}$, and $n+1$ steps. The accuracy of this wave equation can be increase to $O(\alpha^4)$. The accuracy drops when other terms such as viscosity are included, but it still maintain $O(\alpha^3)$. See Chapter19 for an evaluation of the accuracy of various time integration methods, including LF and LFAM3.

LFAM3 has the following advantages and disadvantages over the previously used LF.

- Advantages
  - The accuracy of the time scheme is increased from $O(\Delta t^2)$ to $O(\Delta t^3)$. In particular, it has $O(\Delta t^4)$ accuracy with respect to waves.
  - Computation cost is reduced by 2~30% (see below).
  - Tracer conservation is improved by removing computational mode in LF.
  - Time integration can be restarted from any time step.
- Disadvantages
  - A complete restart requires information at $n-2$, $n-1$, and n steps, making the restart process somewhat complicated and increasing file size. If restart files at $n-2$ and $n-1$ steps do not exist, the calculation starts by treating the restart file at n step as those at $n-2$ and $n-1$ steps.
  - It is always necessary to be aware of whether the current process is being performed during the predictor or corrector substep.

4.3.1　Time integration flow in case of LFAM3

LFAM3 has been the only time integration scheme used in MRI.COM since version 5.0. In this LFAM3, time integration is performed as follows. The items written in bold lines are performed by LFAM3.

Predictor substep

1. Boundary process + Sea ice : Time integration is done by forward differencing to compute $n+\frac{1}{2}$-step external forces.
2. **Evolution of tracers**: To find the pressure gradient at $n+\frac{1}{2}$ step, the tracer values are calculated using an advection scheme with low computational cost (4.7).
3. Equation of state (Section 5.1): Density is calculated from the tracer obtained above. Convective instability is also

checked.

4. **Equation of motion [baroclinic component]**: To find a velocity field at $n + \frac{1}{2}$ step, baroclinic velocity is calculated (4.8).

5. Equation of motion [barotropic component]: Barotropic velocity and sea-surface height at $n + \frac{1}{2}$ and n steps are calculated.

6. Preparation of the corrector substep.

Corrector substep

1. **Evolution of tracer**: Tracer values at $n + 1$ step is calculated with an advection scheme with high accuracy (4.9).

2. Equation of state: Density is calculated from the tracer obtained above. Convective instability is also checked.

3. **Equation of motion [baroclinic component]**: Baroclinic velocity at $n + 1$ step is calculated (4.10).

4. Turbulence closure models: Time integration is done by forward differencing to compute vertical diffusivity and viscosity at $n + 1$ step.

5. Preparing for the next step. The values at $n + \frac{1}{2}$ step are discarded.

SM2005 shows that the maximum allowable time interval of LFAM3 is about 1.8 times as large as that of LF for the wave equation (subsection 23.6.2). If the computational cost of one substep for the predictor or the corrector is the same as the one step in LF, then LFAM3 allows time integration of only $1.8\Delta t$ with the same computational resources as time integration of $2\Delta t$ in LF. However, as mentioned above, the computational cost of LFAM3 is reduced by using less computationally demanding tracer advection scheme and omitting the turbulent closure calculation in the predictor substep, and by omitting the boundary and sea ice process, and barotropic velocity calculations in the corrector substep. Several test cases shows that the adoption of LFAM3 reduces the calculational cost by about 30% due to these effects, and the accuracy of the time integration becomes better.

The details of the calculation process of predictor and corrector substep in MRI.COM are described below.

4.3.2   Evolution of tracers during the predictor step

In the predictor step, the tracer at $n + \frac{1}{2}$ step is calculated only to find the density gradient at $n + \frac{1}{2}$ step. The tracer values at $n + \frac{1}{2}$ step are discarded after the density is obtained.

The predictor step (at $n + \frac{1}{2}$ step) for tracers is written in the form (Fig. 4.3)。

$$\theta^{n+\frac{1}{2}} = \left(\frac{1}{2} - 2\gamma\right)\theta^{n-1} + \left(\frac{1}{2} + 2\gamma\right)\theta^n + (1 - 2\gamma)\Delta t \cdot [\text{Right hand side of the tracer equation(RHS}_\theta)^n], \qquad (4.11)$$

where, the RHS is the sum of θ-tendencies such as advection, diffusion, and surface fluxes. Corresponding to the above equation, the model variable in the b-series are created from linear combinations as described below, rather than using the past values as they are.

- `trcv1b` = $\left(\frac{1}{2} - 2\gamma\right)\theta^{n-1}(\Delta V^T)^{n-1} + \left(\frac{1}{2} + 2\gamma\right)\theta^n(\Delta V^T)^n = \left[\theta\Delta V^T\right]^b$
- `trcbl` = $\left(\frac{1}{2} - 2\gamma\right)\theta^{n-1} + \left(\frac{1}{2} + 2\gamma\right)\theta^n = \theta^b$
- `trcl` = θ^n
- `trcal` = $\theta^{n+\frac{1}{2}}$
- `trcpl` = θ^{n-1} ("p" means "Past".)

Update of `trcbl,trcl`, and `trcpl` is conducted at the end of corrector substep or in `rewrit_prepare`. The `trcpl` should be stored because a new value of θ^{n-1} is needed in the expression (4.20) described below. It is also needed for creating the restart file. (As for u, the value at $n - 1$ steps is not necessary for calculation, but necessary for restart.)

■Modification for the local conservation of tracers   Since the barotropic velocity component (u_m) and sea level height (η) do not satisfy the continuity equation (eq. 6.19), the tracer field cannot satisfy its local conservation, that is, the spatially uniformity of tracer field at the beginning of the predictor substep does not hold at the end of the predictor substep. This situation is rewritten as,

$$\partial_t(\Delta V^T)_{i,j,k-\frac{1}{2}} \neq \frac{\Delta s_{i,j,k-\frac{1}{2}}}{H}\left((\texttt{ws\_total})_{i,j} + (\texttt{transport\_wflux})_{i,j}\right), \qquad (4.12)$$

where `ws_total` is the total amount of water flux entering the grid due to the convergence of both barotropic flow and diffusion of sea level height, and `transport_wflux` is the freshwater flux at the surface. Since the value of $(\theta)^{n+1}$ is used only for the pressure gradient term and is discarded at the end of the corrector step, we need not be concerned about its total
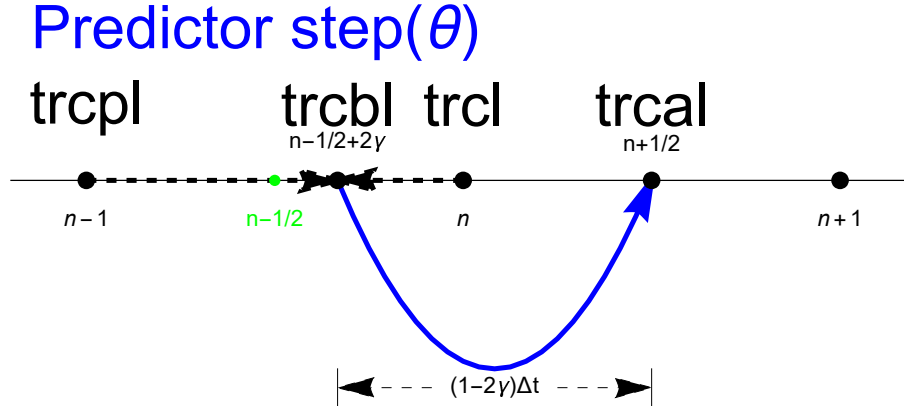
Predictor step(θ)

trcpl   trcbl trcl   trcal

$n-1/2+2\gamma$ $n+1/2$

$n-1$ $n-1/2$ n $n+1$

$(1-2\gamma)\Delta t$

Figure4.3   Schematic of LFAM3 Time integration for MRI.COM. The beginning of the predictor step is a linear combination at $n-1$ and n steps.

conservation of it. On the other hand, the pressure gradient derived from it may have a bad influence on the velocity field when local conservation is not maintained. Therefore, we give up global conservation and consider adding a correction term that resolves the imbalance between the left and right sides of Eq. 4.12.

First, the time evolution of the tracer $\theta_{i,j,k-\frac{1}{2}}$ due to tracer advection is obtained in finite volume as follows.

$$
\begin{aligned}
\left[\theta\Delta V^T\right]_{i,j,k-\frac{1}{2}}^{n+1/2} = &\left[\theta\Delta V^T\right]_{i,j,k-\frac{1}{2}}^{b} \\
&+ (1-2\gamma)\Delta t \left[U^T_{i-\frac{1}{2},j,k-\frac{1}{2}}\theta_{i-\frac{1}{2},j,k-\frac{1}{2}} - U^T_{i+\frac{1}{2},j,k-\frac{1}{2}}\theta_{i+\frac{1}{2},j,k-\frac{1}{2}}\right. \\
&\left. V^T_{i,j-\frac{1}{2},k-\frac{1}{2}}\theta_{i,j-\frac{1}{2},k-\frac{1}{2}} - V^T_{i,j+\frac{1}{2},k-\frac{1}{2}}\theta_{i,j+\frac{1}{2},k-\frac{1}{2}}\right. \\
&\left. W^T_{i,j,k+1}\theta_{i,j,k} - W^T_{i,j,k-1}\theta_{i,j,k-1}\right]^n + \theta^b_{i,j,k-\frac{1}{2}} \times [\text{volume correction term}]
\end{aligned}
\tag{4.13}
$$

$$
\theta^{n+1/2}_{i,j,k-\frac{1}{2}} = \left[\theta\Delta V^T\right]_{i,j,k-\frac{1}{2}}^{n+1/2} / \left[\Delta V^T\right]_{i,j,k-\frac{1}{2}}^{n+1/2}
\tag{4.14}
$$

In this evolution of tracer equation, the following relationship must be satisfied when spatially uniform tracer fields remain to be spatially uniform after the advection.

$$
\begin{aligned}
\left[\Delta V^T\right]_{i,j,k-\frac{1}{2}}^{n+1/2} = &\left[\Delta V^T\right]_{i,j,k-\frac{1}{2}}^{b} \\
&+ (1-2\gamma)\Delta t \left[U^T_{i-\frac{1}{2},j,k-\frac{1}{2}} - U^T_{i+\frac{1}{2},j,k-\frac{1}{2}}\right. \\
&\left. V^T_{i,j-\frac{1}{2},k-\frac{1}{2}} - V^T_{i,j+\frac{1}{2},k-\frac{1}{2}} + W^T_{i,j,k} - W^T_{i,j,k-1}\right]^n + \text{Volume correction term}
\end{aligned}
\tag{4.15}
$$

$$
\begin{aligned}
&\left[U^T_{i-\frac{1}{2},j,k-\frac{1}{2}} - U^T_{i+\frac{1}{2},j,k-\frac{1}{2}} + V^T_{i,j-\frac{1}{2},k-\frac{1}{2}} - V^T_{i,j+\frac{1}{2},k-\frac{1}{2}} + W^T_{i,j,k} - W^T_{i,j,k-1}\right]^n \\
&= \left\{(\texttt{ws\_total})_{i,j} + (\texttt{transport\_wflux})_{i,j}\right\} \frac{\Delta s_{i,j,k-\frac{1}{2}}}{H}
\end{aligned}
\tag{4.16}
$$

Using the above relationship derived from the diagnostic equation of the continuity equation, Eqs. (6.19) and (6.21), the volume change correction term is eventually obtained as follows. (In the corrector step, ΔV^T is obtained so that the correction term is zero.)

$$
\begin{aligned}
\text{Volume correction term} = &\left[\Delta V^T\right]_{i,j,k-\frac{1}{2}}^{n+1/2} - \left[\Delta V^T\right]_{i,j,k-\frac{1}{2}}^{b} \\
&- (1-2\gamma)\Delta t \left\{(\texttt{ws\_total})_{i,j} + (\texttt{transport\_wflux})_{i,j}\right\} \frac{\Delta s_{i,j,k-\frac{1}{2}}}{H}
\end{aligned}
\tag{4.17}
$$

In the notation in the program, the correction term for satisfying local conservation in the predictor step, the last term in

the r.h.s. of Eq. (4.13), is calculated as the quantity θ^b multiplied by this volume correction term as follows

$$\theta^b \times [\text{volume correction term}] = (\texttt{trcbl})_{i,j,k} \left[(\texttt{volt\_vara})_{i,j,k} - (\texttt{volt\_varb})_{i,j,k} \right.$$

$$\left. - (1 - 2\gamma)\Delta t \left\{ (\texttt{ws\_total})_{i,j} + (\texttt{transport\_wflux})_{i,j} \right\} (\texttt{thk\_ratio\_t})_{i,j,k} \right]$$

(4.18)

A similar correction is proposed in SM2005 and corresponds to Eq. (4.8) in SM2005 and Eq. (4.3) in SM2009. However, in SM2005, the layer thickness is modified to achieve local conservation. In MRI.COM, local conservation is realized by modifying the tracer × volume because modifying the layer thickness is quite troublesome.

■Reduction of calculation costs The active tracer (temperature and salinity) values at $n+\frac{1}{2}$ is used only for calculating the pressure gradient through density and discarded after density is obtained. To reduce its computational costs, an advection scheme with low computational costs is used. Calculation of passive tracers are omitted in the predictor substep.

4.3.3 predictor step + baroclinic velocity

In the predictor substep, velocity is calculated as follows (Fig. 4.4).

$$u^{n+1/2} = \left(\frac{1}{2} - 2\gamma \right) u^{n-1} + \left(\frac{1}{2} + 2\gamma \right) u^n + (1 - 2\gamma)\Delta t \cdot [\text{the right hand side of the momentum equation (RHS}_u)^n] \quad (4.19)$$

Here, the density used to calculate the pressure gradient of the RHS_u^n is a linear combination of θ at $n + \frac{1}{2}$, n, and $n - 1$ steps (θ_{filter}).

$$\theta_{filter} = \theta^n + \beta \frac{2\theta^{n+\frac{1}{2}} - 3\theta^n + \theta^{n-1}}{1 - 2\gamma} \quad (4.20)$$

Corresponding to the above equation, the model variables are expressed as follows.

- $\texttt{ubl} = \left(\frac{1}{2} - 2\gamma \right) u^{n-1} + \left(\frac{1}{2} + 2\gamma \right) u^n$
- $\texttt{ul} = u^n$
- $\texttt{ual} = u^{n+\frac{1}{2}}$

The update of $\texttt{ubl}$ and $\texttt{ul}$ is done at the end of the corrector substep in preparation for the next step.
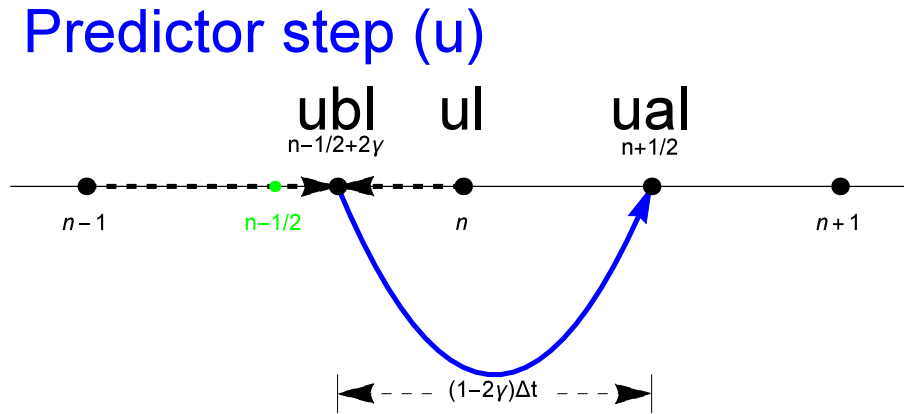

Figure4.4 Schematics of the LFAM3 time step in MRI.COM. The beginning of the predictor substep is at $n - 1/2 + 2\gamma$ step, which is a linear combination of $n - 1$ and n.

Since $u^{n+\frac{1}{2}}$ is used for the advection of tracers, RHS_u^n must be obtained with high precision. The $\texttt{ual}$ obtained here is a provisional value and will be modified after barotropic velocity is obtained.

4.3.4 Barotropic velocity

After the calculation of baroclinic velocity in the predictor substep, the calculation of barotropic velocity is performed to obtain its values at $n + \frac{1}{2}$ step ($U^{n+\frac{1}{2}}$) and at $n + 1$ steps (U^{n+1}) (Chapter 7). The sea level height at $n + 1$ steps (η^{n+1}) can

also be computed here, but in the model η^{n+1} is calculated using the continuous expression $(\eta^{n+1} - \eta^n)/\Delta t = \nabla \cdot U^{n+\frac{1}{2}}$ and $U^{n+\frac{1}{2}}$ in the corrector substep. Actually, the values obtained in the above two methods are identical except for the floating point error.

■Forcing for barotropic component of the equation of motion `zul,zvl`

The forcing (`zul`) should be evaluated at $n+\frac{1}{2}$ step. The component of external forcings such as wind stress are obtained at $n+\frac{1}{2}$ step. Since other components such as advection are obtained at n step, we make an extrapolation with respect to time to make them at $n+\frac{1}{2}$ step. There are several options for this extrapolation.

The first option is the 3rd-order Adams-Bashforth (AB3) method, which has $O(\Delta t^3)$ accuracy. *

$$\texttt{zul}^{n+\frac{1}{2}} = \frac{23}{12}\texttt{zul}^n - \frac{4}{3}\texttt{zul}^{n-1} + \frac{5}{12}\texttt{zul}^{n-2} \tag{4.21}$$

The second option is the quasi-2nd-order Adams-Bashforth (AB2ϵ) method, which does not have $O(\Delta t^2)$ accuracy, but slightly more stable than the AB3 method. This AB2ϵ method is used, for example, to estimate the advection term for the MITgcm. Usually 0.1 is used for ϵ_{AB}.

$$\texttt{zul}^{n+\frac{1}{2}} = \left(\frac{3}{2} + \epsilon_{AB}\right)\texttt{zul}^n - \left(\frac{1}{2} + \epsilon_{AB}\right)\texttt{zul}^{n-1} \tag{4.22}$$

■Calculation of the barotropic component of the equation of motion   The external forcings such as wind stress at the surface at $n+\frac{1}{2}$ step are added to the $\texttt{zul}^{n+\frac{1}{2}}$ obtained above to yield a forcing for the barotropic component of the equation motion without time variation from n to $n+1$ steps. Using the subcycle velocity U^m and the time-filters a_m, b_m (Fig. 4.5) described in Chapter 3 of SM2005, the barotropic velocities are calculated as follows.

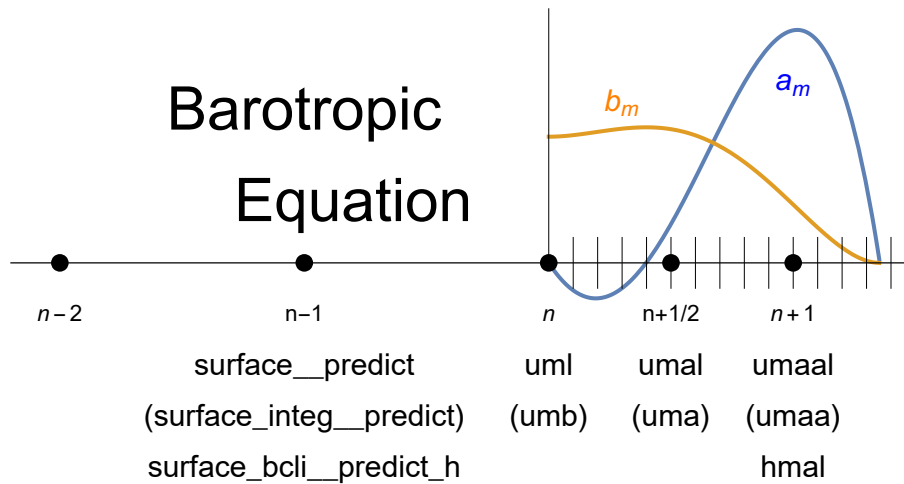Figure4.5   Momentum equation for the barotropic component in MRI.COM in the case of LFAM3 method

$$U^{n+\frac{1}{2}} = \sum^m b_m U^m \tag{4.23}$$

$$U^{n+1} = \sum^m a_m U^m \tag{4.24}$$

$$\eta^{n+1} = \sum^m a_m \eta^m \tag{4.25}$$

$$\tag{4.26}$$

---

* This AB3 method is used in ROMS other than UCLA version

Here,

$$\sum^{m} a_m = 1 \tag{4.27}$$

$$\sum^{m} m\Delta t_{tr} a_m = \Delta t_{cl} \tag{4.28}$$

$$b_{m'}\Delta t_{cl} = \sum_{m=m'}^{m} a_m \Delta t_{tr} \tag{4.29}$$

$$(\eta^{n+1} - \eta^n)/\Delta t_{cl} = \nabla \cdot U^{n+1/2} \tag{4.30}$$

$$(\eta^{m+1} - \eta^m)/\Delta t_{tr} = \nabla \cdot U^{m+1/2} \tag{4.31}$$

The $U^{n+\frac{1}{2}}$ is also used to find the sea level η^{n+1} at $n + 1$ steps using the continuity equation. Therefore, the equation (4.12) holds for $n, n + 1$ steps, and tracers advected by the flow velocity using this barotropic velocity field satisfy local conservation.

The values of $n + \frac{1}{2}$-step and $n + 1$-step in LFAM3 correspond to n-step and $n + 1$-step in LF. When LF was used in the previous MRI.COM, the barotropic velocity values at these times were used separately during the integration of LF from $n - 1$-step to $n + 1$-step and from n-step to $n + 2$-step, respectively. In the case of LFAM3, the barotropic component of equation of motion is calculated only once, and the computational cost of the barotropic component of equation of motion is halved in MRI.COM compared to the case when LF is used.

4.3.5 Corrector substep

Corrector substep (Fig. 4.6) is calculated as follows. The calculation of the corrector substep is no different from that of a normal leap-frog method except for the pressure gradient term, which does not require any special processing such as changing the starting point of the time integration. Only the results of this step are used for subsequent calculations and historical output.

$$\theta^{n+1} = \theta^n + \Delta t \cdot [\text{The right hand side of the tracer equation } (\text{RHS}_\theta)^{n+\frac{1}{2}}] \tag{4.32}$$

$$u^{n+1} = u^n + \Delta t \cdot [\text{The right hand side of the momentum equation } (\text{RHS}_u)^{n+\frac{1}{2}}] \tag{4.33}$$

Here, density used to calculate the pressure gradient of RHS_u^n is a linear combination of θ (θ_{filter}).

$$\theta_{filter} = (1 - \epsilon)\theta^{n+\frac{1}{2}} + \epsilon \left[\left(\frac{1}{2} - \gamma \right)\theta^{n+1} + \left(\frac{1}{2} + 2\gamma \right)\theta^n - \gamma\theta^{n-1} \right] \tag{4.34}$$

The tracer equation is compatible with high precision advection scheme such as SOM because it uses only the n-step tracer values to find the $n + 1$-step values by forward integration. Since the $n + \frac{1}{2}$ value is discarded after the corrector substep, only the values at corrector substep needs to be considered for conservation of the entire system, including the interaction with sea ice and external forces.

4.3.6 Summary of predictor and corrector subcycles

The calculation of the integral from n to $n + 1$ steps when using LFAM3 in MRI.COM is summarized in Fig. 4.7. The renaming of arrays such as trcl is conducted in subroutine rewrit (Fig. 4.7(c) and (e)).

Corrector step (θ)

trcpl trcbl trcl trcal

n−1/2+2γ n+1/2

$n-1$ n $n+1$

Corrector step (u)

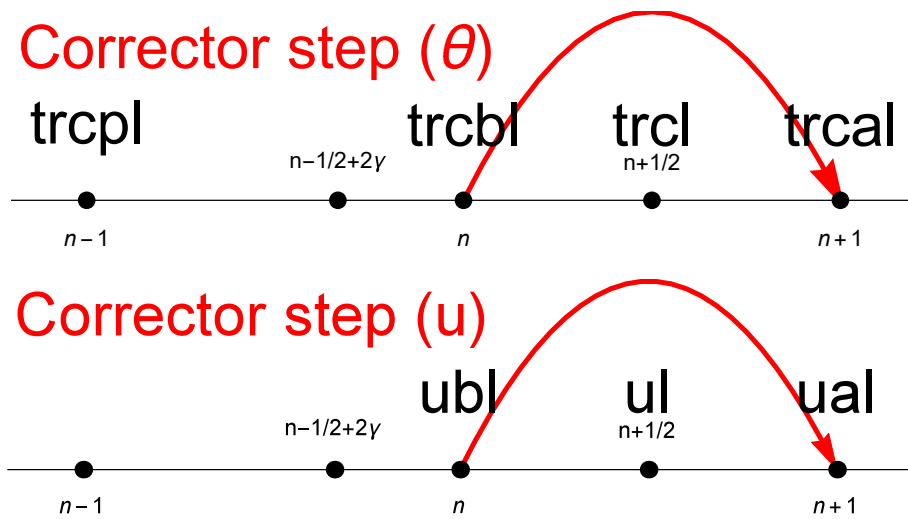ubl ul ual

n−1/2+2γ n+1/2

$n-1$ n $n+1$
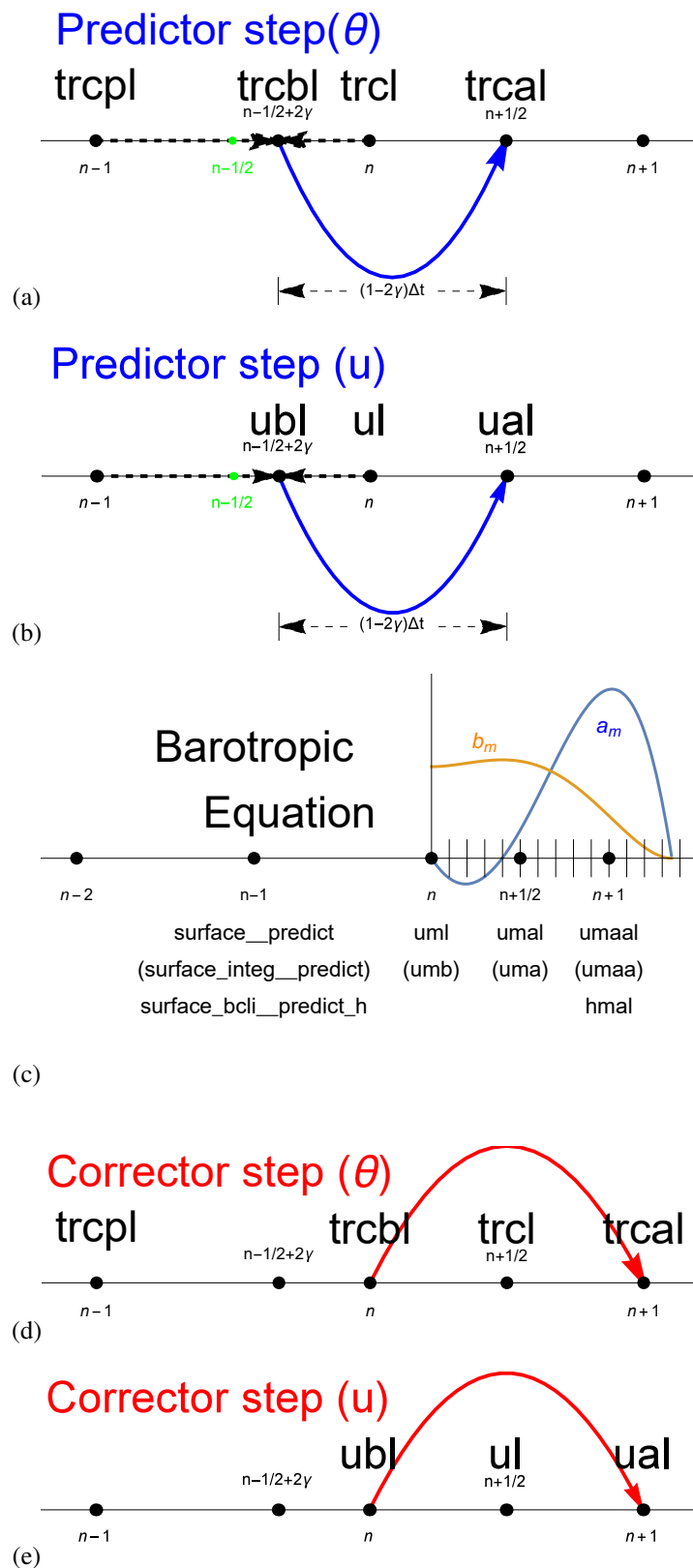
Figure4.6　Time integration of the corrector substep

Figure4.7   Summary of the LFAM3 time integration method in MRI.COM. (a,b) The starting point of the predictor step is $n - \frac{1}{2} + 2\gamma$ step, which is a linear combination of $n-1$ and n steps. Time integration is conducted from $n - \frac{1}{2} + 2\gamma$ step to $n + \frac{1}{2}$ step by $(1 - 2\gamma)\Delta t$. (d,e) In the corrector substep, time integration is conducted from n step to $n + 1$ step using the value at $n + \frac{1}{2}$ step. The values at $n + \frac{1}{2}$ step are discarded after the corrector substep.